Acknowledgements

I thank May-Britt Tessem (supervisor) for giving me the opportunity to work on this project in the ProstOmics group at the department of circulation and medical imaging (ISB). Thank you for your support and motivation. I also thank Sebastian Krossa (co-supervisor), for his guidance and tireless effort in making sure the thesis come to fruition.

I also appreciate the contributions of Elise Midtbust of the ProstOmics group and Kathrin Torseth of the cell and molecular imaging core facility (CMIC).

Kendrick and Bertrand Egharevba, thank you for your patience and understanding.

Abstract

Prostate cancer (PCa) is one of the causes of cancer related deaths in men. The current clinical tools for its diagnosis have limitations that makes it unreliable. Thus, there is need for alternative procedures for PCa diagnosis. Several reports have identified zinc as a potential biomarker for PCa diagnosis. The possiblity of using zinc as a biomarker in PCa identification depends on developing a method for detecting intracellular zinc in prostate tissue. This formed the basis of this project.

Cellular metabolism of the healthy prostate is altered in prostate malignancy. Studies have confirmed that prostate cancer is characterized by decrease in zinc levels compared to healthy prostate. ZIP1 transporter is responsible for the uptake and accumulation of zinc in healthy prostate epithelial cells and its downregulation has been correlated with decreased zinc levels in malignant prostate tissues. Ras responsive element binding protein 1 (RREB1) is a transcription factor that negatively regulates ZIP1 transporter. RREB1 overexpression was found to correlate with ZIP1 downregulation in prostate malignancy.

In this project, intracellular zinc in human PCa tissues were detected using FluoZin-3 zinc indicator dye. The use of FluoZin-3 zinc indicator dye in staining zinc in tissues proved problematic in our experiments. However, by optimizing the fluorescence staining protocol, our results indicate, permeabilizing the tissues before staining with Fluozin-3 zinc dye is an important step. The problem of autofluorescence was encountered in the tissues. The autofluorescence masked specific fluorescence signals and therefore making it difficult to analyze the signals. Sudan Black B and TrueBlack solutions were used to block autofluorescence. Results showed that Sudan Black B reduced autofluorescence but had an impact on the specific fluorescence signals. TrueBlack solution reduced autofluorescence in the tissues.

The presence of ZIP1 and RREB1 proteins in the tissues were determined by labeling with specific primary antibodies. The antibodies were optimized for labeling the prostate tissues to determine the antibody titer that will give a high staining intensity and signal-to-noise ratio (SNR).

Table of content

List of figures

List of tables

Abbreviations

BSA = Bovine serum albumin

DRE = Digital rectal examination

PFA = Paraformaldehyde

PBS = Phosphate buffered saline

PCa = Prostate tissue

PSA = Prostate specific antigen

RREB1 = Ras responsive element binding protein 1

RT = Room temperature

SCBT = Santa Cruz Biotechnology

SLC = Solute carrier

SNR = Signal-to-noise ratio

1. Introduction

1.1. Prostate cancer

Prostate cancer (PCa) is the second most frequently diagnosed cancer among men worldwide after lung cancer and represents the fifth cause of cancer deaths in men [1]. PCa was the most frequently diagnosed cancer among men between 2014-2018 in Norway, representing 27.9% of the new cancer cases recorded [2].

Localized PCa is caused by a malignant growth of cells in the prostate but can metastasize to other parts of the body through the blood stream to form metastases [3]. PCa is often indolent and slow growing but can become aggressive with high proliferation compromising a patient's quality of life and survival. PCa may not have symptoms during its early stages, but at the advanced stages, symptoms include, hematuria, pain in pelvic area, bone pain, trouble urinating [4]. The early diagnosis and prompt treatment of the aggressive types of PCa enhances the chances of survival and quality of life of the patient. However, there's high prevalence of indolent types of PCa and prompt treatment or overtreatment will lead to reduced quality of life due to resultant side effects from treatments. A combination of prostate specific antigen testing (PSA) and digital rectal examination (DRE) are routinely used for PCa screening [4, 5]. However, screening has not been recommended in the Norwegian guidelines. These screening procedures have its limitations and have been criticized for its lack of specificity and sensitivity and its influence on treatment decision making [4]. PCa screening using PSA have led to reduction in mortality from the disease, however, the screening methods leads to overdiagnosis of the cancer. For instance, higher PSA values are also associated with prostatitis (inflammation of the prostate) and benign prostate hyperplasia (enlargement of the prostate). Overdiagnosis results from the detection of some tumors that poses no risk to the patient during his lifetime [6]. These tumors may be clinically insignificant and may not have been diagnosed in the patient's lifetime without screening [7, 8]. Both methods of PCa screening are fallible, hence there is need to identify and develop alternative screening procedures and biomarker for PCa diagnosis. It is established by several studies that the cellular metabolism of the normal prostate epithelia cells is altered in PCa [3, 9]. The normal prostate is characterized by high zinc and citrate levels. In contrast, PCa is characterized by marked decrease in zinc and citrate levels. Zinc, citrate and other biomarkers such as polyamines with their documented altered metabolism and reduction in PCa, can be used in the detection and identification of PCa [5, 9, 10].

1.2. The prostate gland

The prostate is a gland that is part of the male reproductive system located in the pelvic cavity and below the bladder [3]. It consists of smooth muscle fibers and its main function is the production of prostatic fluid which is an important component of the seminal fluid [3, 9]. The prostate gland consists of biologically and histologically different components described as the peripheral zone, central zone, transition zone and the anterior zone (periurethral region) (figure 1) [9, 11]. The peripheral zone constitutes 70% of the prostate's total mass, while the central zone constitutes 25% and the transition zone/periurethral region comprises 5% [9]. The peripheral zone represents the main part of the prostate and it is the major site of prostate carcinoma [3]. Benign prostatic hyperplasia, a condition in which the prostate is enlarged, arise from the transition zone and the central zone [3]. The prostatic fluid is mainly produced in the peripheral zone of the prostate and it contains exceptionally high concentrations of citrate and zinc [9].

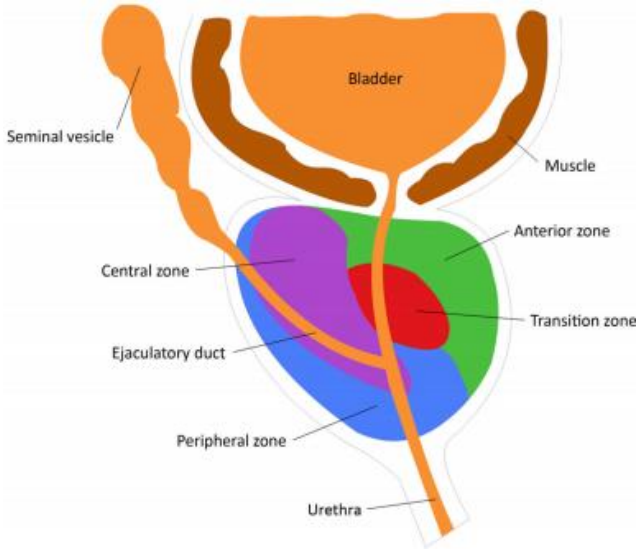

Figure 1. Schematic diagram of different zones of the prostate gland. Taken with permission from Franz et al., 2013.

1.3. Zinc homeostasis and its function in humans

Zinc is an important trace element and the second most abundant trace element after iron in the human body. Zinc biological roles are mainly structural, regulatory and catalytic functions (figure 2) [12]. Dietary zinc is obtained from food sources such as oyster, beans, whole grains, dairy products, red meat and poultry [12]. The human body comprises 2g of zinc, 0.1% is found in the plasma and the

residual found within cells [13]. The highest concentration of zinc is found in the prostate and specific parts of the eye in the human body [3]. Zinc exist either as protein bound or as free zinc ions in cells [13]. Zinc is a cofactor in over 300 enzymes and stabilizes the structure of many proteins, DNA, RNA, as well as signaling enzymes and transcription factors [12, 14]. Of total intracellular zinc, 30-40% is present in the nucleus, while 50% is found in the cytoplasm and the residual 10-20% is associated with the membrane [15]. The function of zinc in human health is multifaceted and includes, cell growth, development, differentiation, maintenance, homeostasis, cell division and connective tissue growth. Zinc also play a role in immune function, bone mineralization, cognitive functions, fetal growth, sperm production and also, maintains normal function of prostate [14]. Deficiency of zinc leads to a plethora of symptoms such as diarrhea, alopecia, loss of appetite, immune system impairment, anemia, growth retardation and neurologic deficits [13, 14, 16]. Zinc deficiency have also been linked with pathophysiological conditions such as cardiovascular disease, depression, neurodegenerative diseases, diabetes mellitus and cancer [13]. Homeostasis of cellular zinc is typically transformed in cancer. The levels of zinc in serum is typically reduced in patients with tumors such as, breast, head and neck, lung, liver, prostate and pancreatic cancer compared to normal serum levels [17]. Accumulation of excess zinc is toxic to the cells except the prostate cells. However, homeostasis of zinc is maintained and regulated by two zinc transporter families; solute carrier 39 (SLC39) (Zip; Zrt, Irt-like proteins) and SLC30 (ZnT) zinc transporters [14]. SLC39 increases intracellular zinc levels by importing zinc into the cells, while SLC30 decreases intracellular zinc by exporting zinc out of the cells (figure 2) [14].

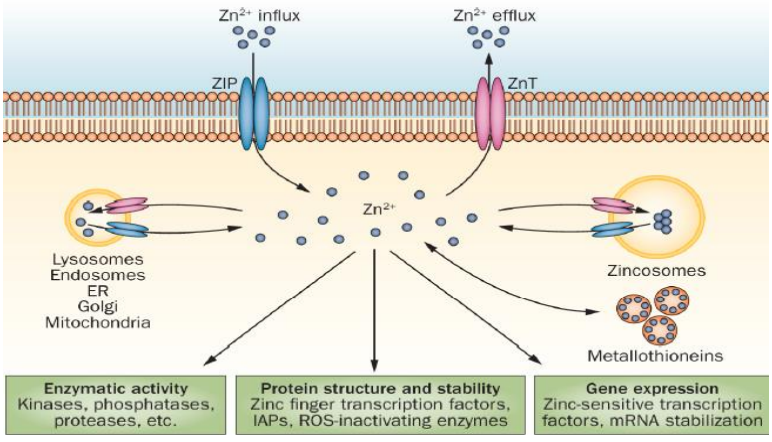

Figure 2. Schematic figure showing the biological roles of zinc and its homeostatic control in the human body. Taken with permission from Kolenko et al., 2013.

1.4. Zinc implication in prostate metabolism and prostate cancer

As mentioned earlier, high concentration of zinc and citrate accumulates in the healthy prostate gland. These are mostly present in the mitochondrial of the prostate's epithelial cells within the peripheral zone [3]. Therefore, healthy prostate is characterized by high zinc and citrate levels, conversely, PCa is characterized by decreased zinc and citrate levels. Decrease in zinc levels have a metabolic effect on prostate cells; due to reduction in zinc levels, zinc is unable to inhibit m-aconitase with the resultant oxidation of citrate and adenosine triphosphate (ATP) production. Therefore, this leads to a transformation of prostate cells from healthy zinc accumulating, citrate producing energy inefficient cells to zinc-deficient citrate- oxidizing malignant energy efficient cells with a functional Krebs cycle (figure 3) [12].

The major function of the prostate gland in humans is the production of prostatic fluid which contains high concentrations of citrate and zinc. With some exceptions, all mammalian cells produce citrate through the mitochondrial synthesis of citrate via the Krebs cycle. The synthesized citrate remains in the mitochondria and utilized via entry into the Krebs cycle. Otherwise, in proliferating cells, mitochondrial citrate is transported out to the cytosol, converted to acetylCoA and utilized for lipid biosynthesis [9]. Contrastingly, in healthy prostate epithelial cells, mitochondrial citrate is not utilized through the Krebs cycle, it is rather transported to the cytosol and secreted into the acini lumen during prostatic fluid production [9]. The non-utilization of citrate via the Krebs cycle by the healthy prostate epithelial cells is due to zinc inhibition of mitochondrial m-aconitase enzyme [9]. In the first step of the Krebs cycle, citrate is oxidized to isocitrate and the process is catalyzed by m-aconitase enzyme (figure 3). Zinc inhibition of m-aconitase enzyme leads to accumulation of citrate in the prostate and citrate is subsequently secreted into the prostatic fluid [3, 9].

The Krebs cycle is important as it helps to meet the energy required for the proper functioning of the cells. In non-prostate cells, zinc cannot inhibit m-aconitase enzyme due to its low levels. Therefore, non-prostate cells produce citrate as an intermediary product of the Krebs cycle, while in prostate cells, citrate is an end-product [3]. Hence, in healthy prostate epithelial cells, the Krebs cycle is abridged leading to a decrease in the main cellular energy supply. The decrease in the cellular energy supply is dangerous to non-prostate cells, but not to prostate cells, which is characteristic of prostatic epithelial cell differentiation [3]. Another physiological significance of high zinc accumulation in prostate cells is, it activates apoptosis and prevents cell proliferation. Effects of zinc on the mitochondria leads to the release of cytochrome c and subsequent activation of caspase resulting in induction of apoptosis leading to inhibition of prostate cells proliferation [18, 19].

PCa is characterized by a remarkable decrease in zinc concentration in the normal prostate peripheral zone [9]. Mawson and Fischer in 1952, were the first to report reduced levels of zinc in PCa [20]. Since then, many clinical studies have corroborated the zinc-prostate cancer relationship [21-23]. Most of the studies have involved the use of zinc staining probes and direct x-ray fluorescence to detect and measure zinc levels in human prostate tissue [24]. The findings of the various studies have been consistent with a decrease in zinc levels in PCa compared to healthy prostate and benign prostate hyperplasia. It has also been revealed that, a decrease in zinc occurs early and precedes the transformation of healthy prostate cells from zinc accumulating citrate producing cells to zinc-deficient citrate-oxidizing malignant cells [24]. And therefore, zinc has the possibility to become an early biomarker in the development of PCa.

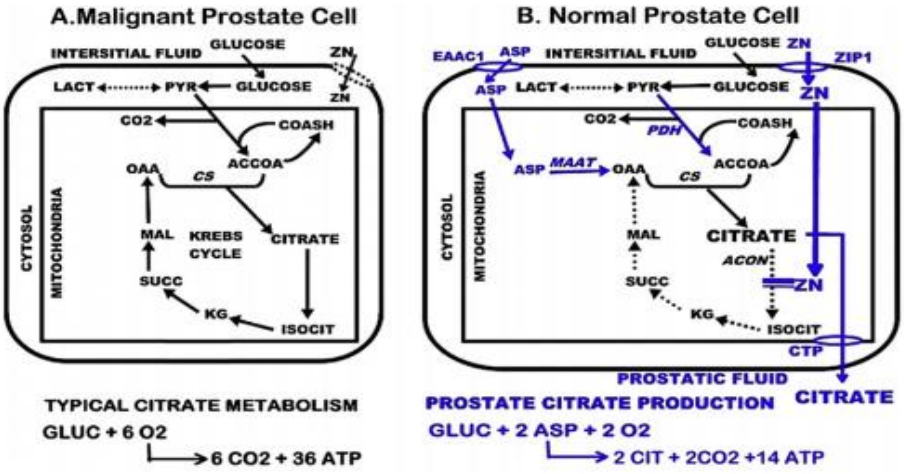

Figure 3. Schematic diagram showing effects of zinc in healthy and malignant prostate epithelial cells. Taken with permission from Costello et al., 2016.

1.5. Zinc transporter proteins and its alteration in prostate cancer

As previously stated, cellular zinc homeostasis is regulated by two families of zinc transporter proteins in humans. The focus here will be on the SLC39 (ZIP) family. The ZIP family member comprises 8 transmembrane domains (TM) with localized extracellular amino (N) and carboxyl (C) termini [3, 25]. The human genome comprises 14 ZIP transporter family encoded by the SLC related genes that have been identified [22, 25].

Several reports have identified ZIP1 as the major zinc transporter protein responsible for zinc uptake and accumulation in prostate epithelia cells [26, 27]. The ZIP1 transporter protein is encoded by the

SLC39A1 gene and have been found to be localized at the basolateral cell membrane of prostate epithelia cells [9]. Studies have shown that increase in zinc uptake and accumulation is correlated with increase in ZIP1 upregulation in normal prostate epithelium and ZIP1 downregulation correlates with decrease in zinc levels in prostate cells [22, 28]. In addition to ZIP1, other SLC transporter proteins such as ZIP2 and ZIP3 have been identified in the apical membrane of healthy prostate cells, where they play a role in zinc reabsorption from prostatic fluid in maintenance of cellular zinc homeostasis [29]. ZIP2 and ZIP3 gene expression have also been reported to be downregulated in PCa [29].

Experimental evidences have established that, ZIP1 gene expression is downregulated in PCa [21]. This explains the mechanism of the loss of zinc and its subsequent decrease in PCa. A downregulated or non-functional ZIP1 transporter protein cannot transport and accumulate zinc in PCa, this results in low levels of zinc in PCa. Decrease in zinc levels means zinc is unable to inhibit citrate oxidation and truncates the Krebs cycle. The resultant malignant cells are zinc deficient and oxidizes citrate and have a functional Krebs cycle. These genetic and metabolic events suggest that both ZIP1 downregulation and subsequent decrease in zinc levels are early events in PCa development. The critical issue is "what mechanism causes the downregulation of ZIP1 transporter protein". Previous studies on prostate cells show that ZIP1 downregulation is due to epigenetic silencing by Ras responsive element binding protein-1 (RREB1) [30, 31].

RREB1 is a zinc finger transcription factor that activates or represses gene transcription depending on the promoter which it binds [30]. The ZIP1 promoter comprises a cis-acting element, that contains a consensus sequence which RREB1 binds [30]. RREB1 represses ZIP1 gene expression. RREB1 acts on ERK as an effector, downstream of the Ras pathway as shown in figure 4. Reports shows that, the Ras pathway is overexpressed in PCa and that zinc is also a negative regulator of the pathway by inhibiting Ras signaling [30, 32, 33]. RREB1 is activated and regulated by the Ras pathway. Thus, activation of Ras pathway in PCa would lead to overexpression of RREB1 and therefore ZIP1 downregulation and resultant decrease in zinc levels in PCa [31].

These genetic events (RREB1 overexpression and decrease in ZIP1 gene expression) coupled with the metabolic events (decrease in zinc levels) are changes that occur early in the development of PCa as shown by experimental studies and reports [30, 31].

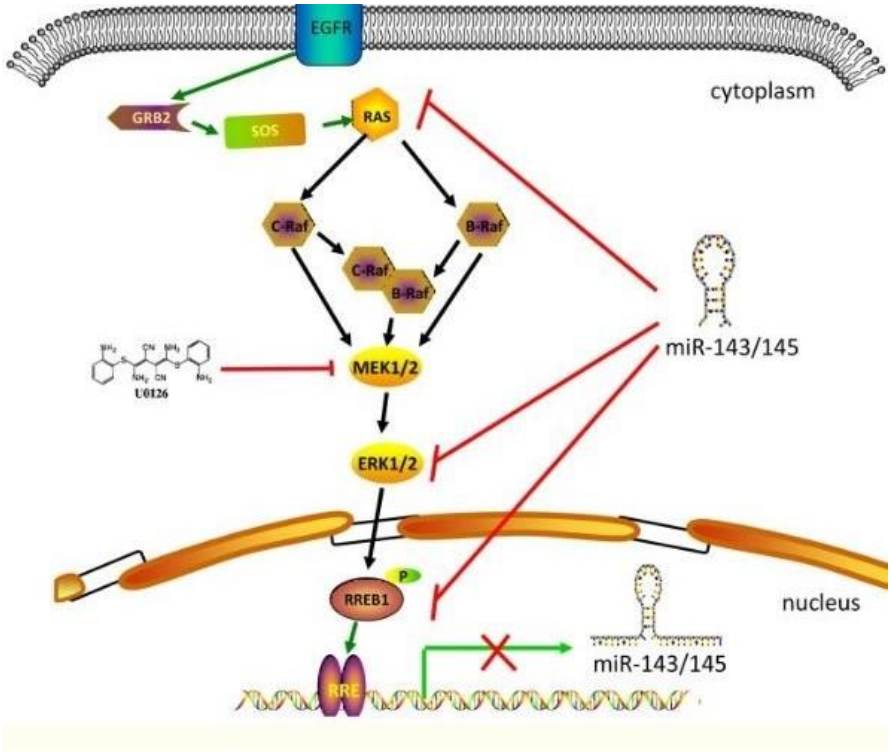

Figure 4: Schematic diagram showing RREB1 as a downstream effector of Ras pathway. Taken with permission from Deng et al., 2020.

1.6. Immunofluorescence staining

Immunofluorescence is an immunostaining method that is used to detect the distribution and localization of diverse proteins in different types of tissues or cells using specific antibodies. Immunofluorescence makes it possible to amplify signals and gives exceptional sensitivity in comparison to immunohistochemistry. Many components in a tissue can be visualized with immunofluorescence staining through combinations of specific antibodies that is conjugated to a fluorescent dye [34].

Direct and indirect immunofluorescence are two methods employed in immunofluorescence staining. The two methods can be distinguished on the basis that, whether the fluorescent dye is conjugated to the primary or secondary antibody. In the direct immunofluorescence, primary antibody is conjugated directly to a fluorophore (fluorescent molecule). The primary antibody binds the target antigen and the conjugated fluorophore can be detected by a microscope (figure 5). This method is quick as it requires only one labeling step. Conjugated primary antibody is expensive compared to secondary antibody, making indirect immunofluorescence staining technique a cheaper option. Indirect immunofluorescence involves the use of two antibodies, a primary antibody that binds the

target protein (unconjugated) and a secondary antibody that is tagged with a fluorophore. The secondary antibody binds the primary antibody and therefore the target protein already bound by the primary antibody is detected with the aid of a microscope (figure 6). Indirect immunofluorescence is less expensive, but time-consuming due to additional labeling steps and generally lead to signal amplification [34, 35].

Indirect immunofluorescence can also be used in the double staining of tissues. This involves the use of two different primary antibodies that have been raised in different species (rabbit and mouse) and two different secondary antibodies conjugated to two different fluorescent dyes that can be monitored in two different channels. Double labeling of tissues allows comparison in the distribution of specific target protein with another target protein in the same tissue. It also helps understand the spatial relationship between two different proteins in the same tissue [36].

Tissue fixation in immunofluorescence staining is a crucial step as it preserves morphology, prevents autolysis, and helps to preserve cellular distribution of antigens and retain antigenicity. Tissue fixation can be done by using chemical fixatives such as cross-linking fixative reagents or organic solvents. Formaldehyde and glutaraldehyde are examples of cross-linking fixative reagents that cross-links adjacent proteins after binding cellular and tissue components. Methanol and acetone are examples of organic solvents that remove lipids, dehydrate cells, denatures and precipitate cellular components [34]. Organic solvents cause damages to cell morphology, but are overall relatively mild chemical fixatives and can be used to maintain antigens that are easily altered by aldehyde fixation [37].

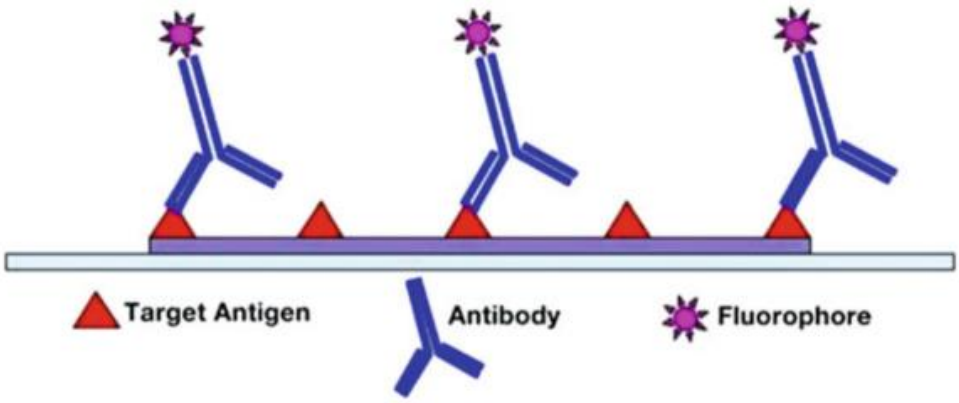

Figure 5. Schematic figure of direct immunofluorescence. Taken with permission from Kyuseok et al., 2019.

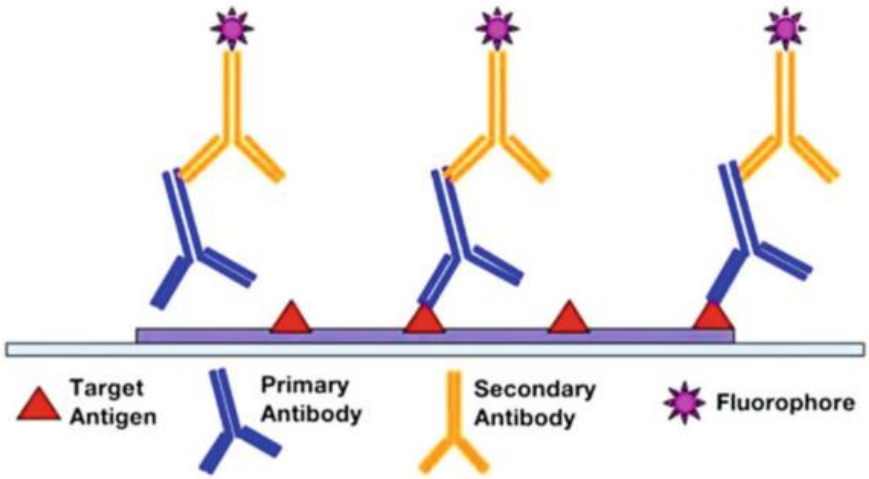

Figure 6. Schematic showing indirect immunofluorescence. Taken with permission from Kyuseok et al., 2019.

1.7. Principles of fluorescence

The fundamental principle of fluorescence involves the ability of a fluorescent dye to absorb (excitation) light energy (photons) at one wavelength and the emission of parts of the light energy at another wavelength [38, 39]. The light emission process takes place a few nanoseconds after light absorption (excitation) and this is known as fluorescence [38]. The photon energy emitted usually has less energy than the one absorbed by the fluorescent dye. This process can be illustrated by the Jablonski energy diagram (figure 7) [40]. The electrons of a fluorescence molecule are usually at the ground state (S_0) before excitation. The absorbed photon energy by a fluorescence molecule, causes its electrons to move from the ground state (S_0) to the next excited states (S_1-S_2). The excited state electron loses its excess energy to heat, by collision with nearby molecules or through vibrational relaxation and internal conversion and return to the ground state (S_0), emitting photons with lower energy. Therefore, the emitted photon has lower energy and a longer wavelength that corresponds to a different colour [38, 39, 41]. Hence the emitted light (fluorescence) has a lower energy, but a longer wavelength. Conversely, the absorbed light has a higher energy and a shorter wavelength. This differences in wavelength and energy level is known as the Stokes shift. Stokes shift is the difference between the maximum absorption and emission peaks in wavelength [38, 41] (figure 8). The larger the Stokes shift, the better the signal separation and less interference from excitation light [38]. The fluorescence intensity and efficiency of a fluorescence dye can be determined by its Quantum yield value. The Quantum yield of fluorescence is the ratio of the emitted photons to the absorbed photons. The higher the quantum yield value, the better the fluorescence effectiveness and intensity [38, 41].

Therefore, a fluorescent dye with a high quantum yield and large Stokes shift will be suitable for scientific studies.

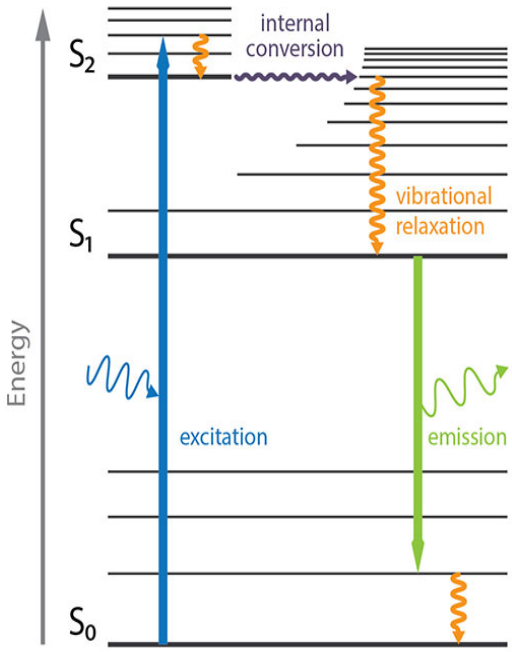

Figure 7. Transition in the energy state of fluorescence molecule depicted by Jablonski energy diagram. Taken from Enzolifesciences Technotes, 2019.

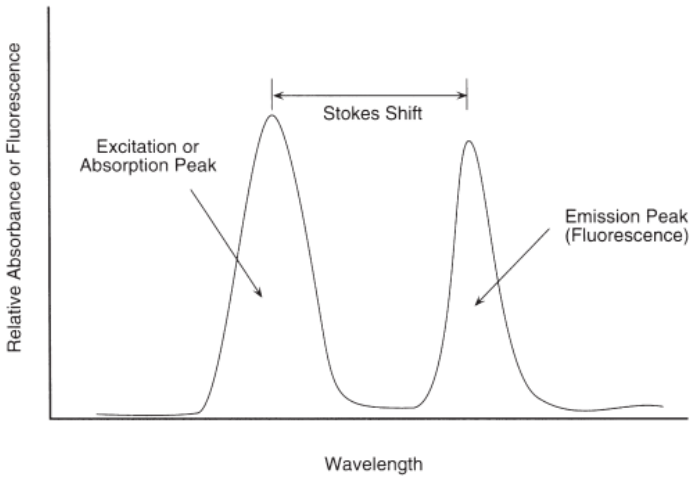

Figure 8. Fluorescence spectrum showing the distance between the excitation wavelength and emission wavelength (Stokes shift). Taken from Hermanson., 2013.

1.8. Qupath image analysis software

Qupath is a free and open source bioimage analysis software designed for whole slide image analysis. It is used to view images, manually annotate or draw region of interests, manually count cells, detection of cells and classification [42]. Qupath cell detection tool makes it easier to automate, detect and count cells that are either positive or negative to a stained marker. The cell detection tool is used by manually drawing around the region of interests in a sample using the drawing tools of Qupath such as the polygon tool to create annotations and run. Qupath detects the cells within the annotations and calculate the number of stained cells within each annotation as shown in figure 9.

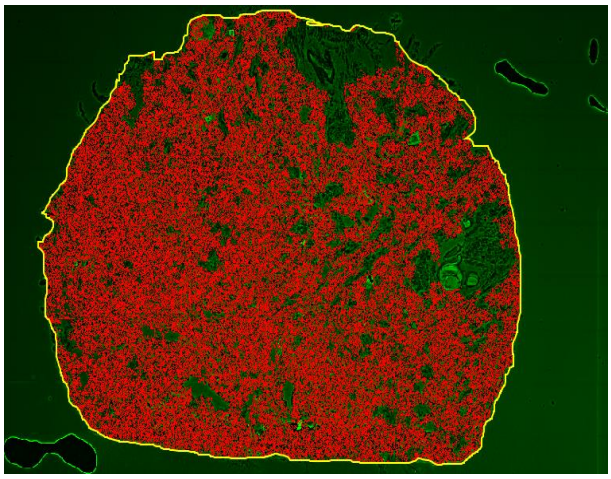

Figure 9. Diagram showing Qupath image analysis. Yellow line represents annotation drawn with Qupath polygon tool and the red spots shows cells detected with Qupath's Analyse/cell detection command.

1.9. Aims of project

The goal of this project is to establish and evaluate fluorescence staining protocol of prostate tissue to detect the presence of zinc and its pathway proteins (ZIP1 and RREB1). This will be done by optimizing a protocol for the single staining of zinc, ZIP1 and RREB1 in prostate tissue. The protocol will also include optimization of the background fluorescence with Sudan Black B incubation times, solvent optimization, and prevention of non-specific antibody binding with bovine serum albumin (BSA). Furthermore, double immunostaining of ZIP1 and RREB1 proteins will be evaluated.

2. Materials and methods

Fresh frozen prostate tissue cores were drilled from whole-mount prostate slices from prostatectomy patients collected by Biobank 1 and used for this project. All patients gave informed consent and study is approved by the regional ethical committee of Mid-Norway (2017/576). The whole-mount slices and drilling procedure of cores were kept frozen during processing and the cores were stored at –80 °C as described by Bertilsson et al [43] . Tissue sections to be used for staining zinc and other proteins were cryo-sectioned in 10 µm sections (3 mm diameter sampled from human tissue) and then mounted unto microscope glass slides.

- Trace metal free containers/bottles (plastic materials). Plastic containers were chosen over glass containers to avoid contamination of samples with trace metals. Acid washed glass containers can also be used [44].
- Phosphate buffered saline (PBS) tablets (Dulbecco A) pH 7.4 (Oxoid, ThermoFisher Scientific).
- 4% Paraformaldehyde (PFA) (ThermoFisher Scientific).
- Ultrapure water used for preparing PBS and as a diluent for isopropanol and ethanol.
- 1% Bovine serum albumin (BSA) in PBS pH 7.4 (Blocking and Antibody dilution solution) (Sigmaaldrich).
- Sudan Black B powder (Sigmaaldrich 199664).
- TrueBlack Lipofuscin Autofluorescence Quencher (Biotium 23007).
- TrueBlack Background Suppressor system (Biotium 23012A).
- TrueBlack Background Blocking Buffer (Biotium 23012B).
- Fluozin-3-AM ester (Zinc probe) (Thermo Fisher Scientific F24195): 1 mM Stock solution in anhydrous Dimethyl sulfoxide. 1 µM Fluozin-3 in PBS pH 7.4 was used in staining zinc in tissue sample.
- Primary and secondary antibodies used are presented in Table 1.

Table 1: list of primary and secondary antibodies.

Antibody	Stock concentration	Manufacturer's name
ZIP1 antibody (Rabbit IgG Polyclonal) (extracellular only against isoform I)	0.8 mg/ml	Thermo Fisher scientific PA5-77766
RREB1 antibody (Rabbit IgG Polyclonal)	0.1 mg/ml	Thermo Fisher Scientific PA5-65129

Anti-ZIP1/SLC39A1 Rabbit IgG Antibody	1 mg/ml	Abcam ab105416
Mouse IgG Anti ZIP1 (F-2)	0.2 mg/ml	Santa Cruz Biotechnology (SCBT sc-393345)
Isotype control (Rabbit IgG Isotype control)	5 mg/ml	Thermo Fisher Scientific 02-6102
647_ Anti Rabbit; (Goat-anti-Rabbit-IgG-H-L-Highly crossed adsorbed secondary antibody-Polyclonal)	2 mg/ml	Thermo Fisher Scientific A32733
Anti-Mouse m-IgGk BP-CFL 488 (secondary antibody)	0.4 mg/ml	SCBT sc-516176

- Isopropanol (2-propanol Fluka Analytical 34965-1 L).
- Ethanol (Rectapur Ethanol 96%, GPR VWR 20824.296).
- Antifade mounting medium with DAPI (Vectorlabs).
- Fluorescence microscope
- Tissue-Tek slide holder and slide dish. Both were used during the washing step. The slide holder was used in holding tissue mounted on a microscope glass slide in position, for immersion in washing solution contained in a slide dish.
- Humidified slide chamber (contained PBS) was used to hold slides during staining and it provides humid environment which prevents the tissue samples from drying out during incubation.

2.1. Overview of methods

2.1.1 Preparation of reagents

The different reagents and solutions used for this project were prepared as described below:

Preparation of 1x PBS and 1% BSA

1x PBS (pH 7.4)

1 tablet per 100 ml of ultrapure water.

1% BSA solution

1 g of BSA powder was added to 100 ml PBS pH 7.4.

Preparation of 0.25% Sudan Black B solution in 70% Isopropanol

Sudan Black B (0.25 g) was added to 100 ml 70% Isopropanol (30% ultrapure water). The mixture was stirred overnight at room temperature. Non- solubilized particles were removed by centrifugation at 3000 xg for 20 minutes and filtered through 4-7 µm filter. The solution was stored in the dark for no longer than 4 weeks.

Preparation of 0.25% Sudan Black B solution in 70% ethanol

Sudan Black B (0.25 g) was added to 100ml 70% ethanol (30% ultrapure water). The mixture was stirred overnight at room temperature. Non- solubilized particles were removed by centrifugation at 3000 xg for 20 minutes and filtered through 4-7 µm filter. The solution was stored in the dark for no longer than 4 weeks.

Preparation of1X TrueBlack solution in 70% ethanol

TrueBlack solution (20X) was diluted to 1X in 70% ethanol before use. TrueBlack solution (50 µl) was added to 1 ml 70% ethanol and vortex to mix properly.

2.1.2 Single staining of zinc in prostate tissue using Fluozin-3 zinc dye and optimization of background fluorescence with Sudan Black B solution

Background autofluorescence can interfere with immunofluorescence staining and analysis, hence there is need to reduce or eliminate it. One of the approaches used to eliminate background autofluorescence, is the use of Sudan Black B dye. In this experiment, an untreated tissue slide was used as a control. The control (untreated) is a tissue sample stained with Fluozin-3 zinc indicator dye but without Sudan Black B incubation. The experiment was performed as follows:

Tissue samples were taken out of the –80 °C freezer and dried for approximately 15 minutes. The tissues were fixed with 500 µl of 4% PFA solution for 15 minutes at room temperature (RT) and washed twice in 1 x PBS pH 7.4 for 5 minutes at RT after fixation. Afterwards, tissues were incubated in 0.25% Sudan Black B solution for 0, 10, 30 and 60 minutes. At the end of each incubation time, the tissues were washed twice in PBS pH 7.4 for 2 minutes at RT. At 0 minutes incubation time, tissues were overlay with Sudan black B dye and quickly washed in PBS pH 7.4. Tissues were stained with 200 µl of 1 µM FluoZin-3 zinc probe in 1 x PBS pH 7.4 (1:1000) for 60 minutes in the dark at RT and slides were kept in a humidified chamber containing PBS and thereafter, washed twice in PBS pH7.4 for 2 minutes at RT, avoiding light exposure.

DAPI containing mounting medium was added dropwise unto the tissue and mounted with a cover slip prior to imaging. The images were captured with a fluorescence microscope using the same settings/parameters for all images as shown in table 2.

2.1.3. Optimization of background fluorescence with TrueBlack Autofluorescence quencher

The quenching of the background fluorescence with Sudan Black B dye in 70% isopropanol and ethanol resulted in minimal background fluorescence. However, specific signal from the Fluozin-3 zinc indicator dye was affected. Thus, other background fluorescence blocking reagent (TrueBlack Autofluorescence quencher) was used to improve the background fluorescence and subsequently preserve the signal from zinc staining. The experiment was performed as described below:

Tissue samples were taken out of the freezer –80 °C and dried for approximately 15 minutes at RT. The tissues were fixed with 4% PFA for 15 minutes at RT and thereafter washed twice in PBS pH 7.4 for 1 minute at RT. Excess PBS was drained without allowing the sections to dry out. The slides were placed in a humidified slide chamber and tissue section overlay with 200 µl 1x TrueBlack solution in 70% ethanol (except the control slide). The slide (treated with 1x Trueblack) was incubated for 1

minute and then washed three times in PBS 7.4 at RT. The slides were then mounted with cover slip after adding DAPI antifade mounting medium. The slides were scanned with a fluorescence microscope using the same settings/parameters.

2.1.4. Single staining of zinc without fixation

The signal obtained from staining of zinc in the tissue with Fluozin-3 zinc dye in the previous experiments was either minimal or not detected in some tissues. In an attempt, to improve the signal and optimize the single staining of zinc in the tissue, the tissue was not fixed with 4% PFA and permeabilization of tissue was performed, respectively. Both experiments are described in this section and section 2.1.5 respectively.

The experiment was done as described in section 2.1.2 above but without the fixation step. The Sudan Black B dye incubation was replaced with TrueBlack in 70% ethanol incubation (section 2.1.3) also without the fixation step.

2.1.5. Single staining of zinc in permeabilized tissue

The tissue was fixed and washed as described in section 2.1.2. Tissue section was then covered with 25 µl TrueBlack Background Blocking Buffer (permeabilizing) and incubated in a humidified chamber containing PBS for 10 minutes at RT. Before incubation, tissue sections were covered with parafilm to spread the blocking buffer solution over the sample. After incubation, sample was removed from wash buffer and excess wash buffer drained. Excess wash buffer was carefully drained to prevent sections from drying out. The tissue section was stained with 200 µl of 1 µm FluoZin-3 zinc indicator dye dissolved in TrueBlack Background Blocking Buffer. Thereafter, incubated in the dark in a humidified chamber containing PBS for 60 minutes at RT. Slide was then washed in PBS pH 7.4 for 1 minute at RT. Tissue section was further treated as described from the seventh paragraph of section 2.1.3.

2.1.6. Single staining of ZIP1 proteins (indirect immunofluorescence staining) and blocking optimization.

Background fluorescence in tissues can emanate from tissue autofluorescence or non-specific binding of antibody. Binding of non-specific proteins in the tissues can be reduced by using blocking solution such as bovine serum albumin (BSA). In this experiment, 3 different incubation times (0, 10 and 30 minutes) were tested to determine the optimal blocking incubation time. The experiment was performed as described below:

The tissues were fixed with 500 µl of 4% PFA solution for 15 mins at room temperature and washed twice in 1x PBS pH 7.4 for 5 mins after fixation. The tissues were blocked by incubation in 300 µl of blocking solution (1% (w/v) BSA in 1 x PBS pH 7.4) for 0, 10 and 30 minutes in a humid chamber at RT (optimal blocking time tested).

The primary antibody (ZIP1 ThermoFisher) was diluted in 1% blocking solution (optimal antibody dilution tested). The tissues were covered with 300 µl of primary antibody and incubated in a humid chamber for 60 minutes at RT. Thereafter, tissues were washed 3 times in PBS pH 7.4 for 2 minutes at RT. The secondary antibody was diluted in PBS pH 7.4 (1:1000). The tissues were incubated in 300 µl of secondary antibody for 60 mins in a humidified slide chamber at room temperature. Tissues sections were washed twice in PBS pH 7.4 for 2 minutes at room temperature avoiding light exposure.

DAPI containing mounting medium was added dropwise unto the tissue and mounted with a cover slip prior to imaging. The images were captured with a fluorescence microscope using the same settings/parameters for all images as shown in table 2.

2.1.7. Single staining of ZIP1 with two other Anti-ZIP1 antibodies

Anti-ZIP1 antibodies from abcam and Santa Cruz Biotechnology (scbt) were tested for the single staining of ZIP1. Antibody dilutions 1:50, 1:100 and1:500 was tested for abcam, while 1:50, 1:500 was tested for scbt. The test was performed as described in section 2.1.6, except TrueBlack Background Suppressor was used as the blocking solution and antibody dilution solution. Furthermore, 25 µl TrueBlack Background Suppressor was used to cover tissue sections and incubated at RT for 10 minutes. Prior to incubation tissue sections were covered with parafilm to spread TrueBlack Background Suppressor solution over the tissue sections and thereafter incubated in a humidified chamber to keep sections from drying out. The samples were then incubated in Anti-ZIP1 antibody

(abcam or scbt) diluted in TrueBlack Background Suppressor for 1 hour at RT. The samples were then rinsed twice briefly and washed 3 times for 5 minutes in PBS and then rinsed again twice in PBS. Secondary antibody diluted in TrueBlack Background Suppressor was added to the tissue sections and incubated for 1 hour (protected from light). Anti-Rabbit secondary antibody dilution 1:200 was used for abcam Anti-ZIP1 antibody signal detection, while Anti-Mouse secondary antibody dilution 1:50 was used for scbt Anti-ZIP1 antibody. Samples were then rinsed twice and washed 3 times for 5 minutes in PBS (protected from light) and then rinsed again twice in PBS. The slides were then treated with TrueBlack autofluorescence quencher in 70% ethanol as described in section 2.1.3 from the seventh paragraph. The same procedure was also used for the secondary antibody labeled tissue test without primary antibody. Slides were then captured with a fluorescence microscope.

2.1.8. Single staining of RREB1 proteins

The labeling of RREB1 proteins in tissues was carried out as described in section 2.1.7. Anti-RREB1 antibody dilutions of 1:50 and 1:500 was tested.

2.1.9 Double staining of ZIP1 and RREB1 proteins in tissues

For double staining of proteins in tissues it is important to use two primary and secondary antibodies from different species. Thus, in this experiment Anti-ZIP1 antibody (mouse) (scbt) at a dilution of 1:50 and Anti-RREB1 antibody (rabbit) at a dilution of 1:50 were used for the double labeling of both proteins. Likewise, the secondary antibodies used were Anti-Rabbit (1:200) and Anti-Mouse (1:50) (Table 1). Both primary antibodies were mixed prior to staining. Similarly, the secondary antibodies were also mixed. The experiment was performed as follows:

Tissue samples were taken out of the –80 °C freezer and dried for approximately 15 minutes. The tissues were fixed with 500 µl of 4% PFA solution for 15 minutes at room temperature (RT) and washed twice in 1 x PBS pH 7.4 for 5 minutes at RT after fixation. TrueBlack background suppressor was used as antibody diluent and blocking solution. 25 µl TrueBlack Background Suppressor was used to cover tissue sections and incubated at RT for 10 minutes. Prior to incubation tissue sections were covered with parafilm to spread TrueBlack Background Suppressor solution over the tissue sections and thereafter incubated in a humidified chamber to keep sections from drying out. The samples were then incubated in primary antibody mixture (100 µl) diluted in TrueBlack Background Suppressor for

1 hour at RT. The samples were later rinsed twice briefly and washed 3 times for 5 minutes in PBS and then rinsed again twice in PBS. Secondary antibody mixture (100 µl) diluted in TrueBlack Background Suppressor was added to the tissue sections and incubated for 1 hour (protected from light). Samples were then rinsed twice and washed 3 times for 5 minutes in PBS (protected from light) and then rinsed again twice in PBS. The slides were then treated with TrueBlack autofluorescence quencher in 70% ethanol as described in section 2.1.3 from the seventh paragraph.

2.2. Fluorescence microscopy

The same settings were used for all the fluorescence images captured, to achieve easy comparability between the images.

Table 2: Fluorescence microscope settings used for capturing slide images

Emission wavelength	455 nm (DAPI), 670 (CY5), 518 nm (FITC), 565 nm (CY3)
Exposure time	20ms (DAPI), 250ms (FITC), 250ms (CY5)
Numerical Aperture	0.75
Magnification	20 x
Objective working distance	600 µm
Lamp intensity (Reflected)	92.00%
Lamp intensity (Transmission)	9.00 V
Gain	0.00dB

2.3. Image analysis

The images were captured by fluorescence microscope and analyzed with Qupath`s algorithm as discussed in section 1.8 and subsection 2.3.1 [42]. In fluorescence staining protocol, the staining quality and signal-to-noise ratio (SNR) is instrumental in determining the performance of the basic or optimized staining protocol. Thus, we calculated the mean fluorescence intensity (average staining intensity) and the signal-to-noise ratio (SNR) to determine the fluorescence images with the highest staining intensity (mean fluorescence intensity) and SNR. This is important for easy comparability among images obtained from staining the tissues. The calculation of both parameters is presented in the next sections.

2.3.1. Calculation of average intensity

Qupath was used to calculate the mean fluorescence intensity of the images. The values obtained represents the average of the mean fluorescence intensity of each detected cell, hereafter referred to as the average intensity. To calculate average intensity of the far-red channel that corresponds to the primary/secondary antibody binding to the tissue, the fluorescence image of the tissue section was first annotated by drawing a circle around the image using the polygon tool command of Qupath (figure 9). Afterwards, set parameters such as detection channels (FITC, CY3, CY5, DAPI), score compartment (nucleus or cytoplasm) and then run. The average intensity was calculated using the Analyze/Cell detection command of Qupath algorithm. The values for the average intensity were obtained from the measure/show detection measurement command of Qupath algorithm. The mean background intensity was calculated using the same method as the fluorescence mean intensity calculation, albeit on a far-red channel that correspond to tissue without antibody staining. The background value was subtracted from each average intensity values. Background subtraction is necessary to eliminate any unspecific signal that may arise due to autofluorescence or introduced during image scanning by fluorescence microscope.

2.3.2 Calculation of signal-to-noise ratio

Signal-to-noise ratio (SNR) is a parameter that can be used to assess the quality of images. It can also be used to assess the performance of microscope detectors [45]. SNR is also used in other field such as in engineering. Therefore, SNR have different definitions and interpretations depending on the context. The signal here refers to the FluoZin-3 signal or fluorophores (primary/secondary antibody) used to stain the tissues, while the noise is the background signal which occur due to autofluorescence or unspecific binding of antibody.

The SNR was calculated as the ratio of the average signal intensity divided by the standard deviation of the background.

3. RESULTS AND DISCUSSION

3.1. single staining of zinc and optimization of background fluorescence

Background fluorescence quenching with Sudan Black B dye resulted in a decrease in the specific fluorescence signal as the Sudan Black B incubation time increases from 0-30 minutes (Figure 10a). Sudan Black B incubation at 10 and 30 minutes resulted in less background fluorescence compared to incubation at 0 minute as seen on the image in Figure 10a. However, Sudan Black B incubation at 10 and 30 minutes had effect on the specific Fluozin-3 zinc staining as it reduces the staining intensity of the zinc probe, making it almost invisible. Furthermore, Sudan Black B incubation at 10 and 30 minutes had a higher signal-to-ratio than incubation at 0 minutes as shown in Table 3. The SNR shown in table 3 was calculated as described in section 2.3.2 above. The untreated sample (control) was characterized by significantly high background fluorescence albeit with a signal-to-noise ratio only better than incubation time of 0 minutes (Figure 10c, Table 3). This was expected as autofluorescence was not blocked in the tissue. At 0 minutes incubation time, the tissue was incubated in Sudan Black B and quickly washed off. Thus, the specific signal is indistinguishable from the autofluorescence. Interestingly, the images (Figure 10a) were characterized by wavy like structures and dark particles. The dark particles may have originated from the Sudan Black B treatment. Sudan Black B incubation time of 60 minutes resulted in a staining pattern in which specific Fluozin-3 zinc probe signal is more visible, but with a lower signal-to-noise ratio than incubation times of 10 and 30 minutes. However, the specific signal observed, appears to include background autofluorescence.

The image histograms depict the distribution of the pixel intensity in the fluorescence images (Figure 10b, c). Images consists of pixels and the shape of the image histogram provides necessary information regarding the quality of the image. The image histogram (Figure 10b) shows that the pixels in the images are not evenly distributed and the pixels are distributed in the right side (lower end of the dynamic range) of the histogram. Hence the fluorescence images for 0, 10, 30 minutes incubation times appear darker with poor contrast. The image histogram of the untreated sample and 60 minutes incubation time shows pixel distribution with a better spread in the pixel dynamic range the other incubation times. Hence, both images appear slightly brighter than others (Figure 10b, c).

(a)

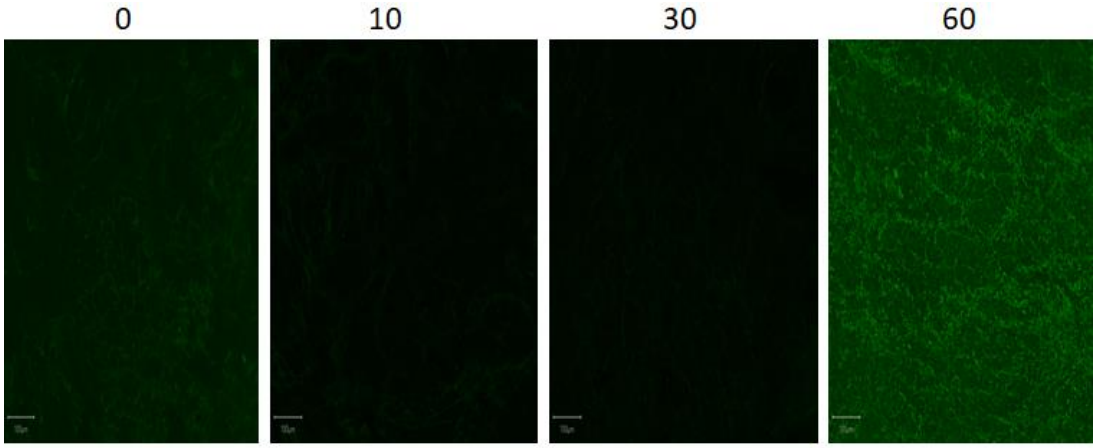

(b)

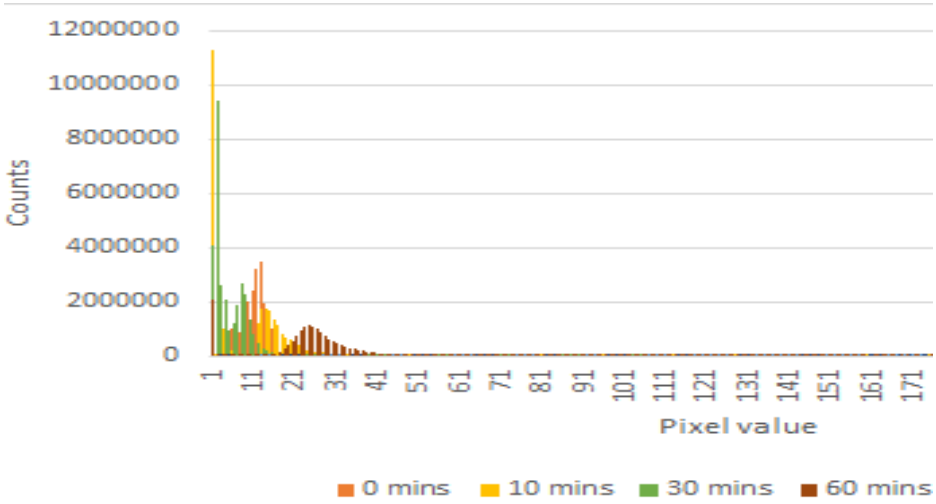

Figure 10. a. Fluorescence image showing quenching of background autofluorescence using Sudan Black B solution using 4 different times (20x magnification). The green channel represents Fluozin-3 zinc dye signal. O represents Sudan Black B incubation of 0 minutes, 10 represents 10 minutes incubation time, 30 represents 30 minutes incubation time and 60 represents 60 minutes incubation time. b. corresponding image histograms showing distribution of pixels for the different incubation times respectively. Scale bar= 100 µm.

(c)

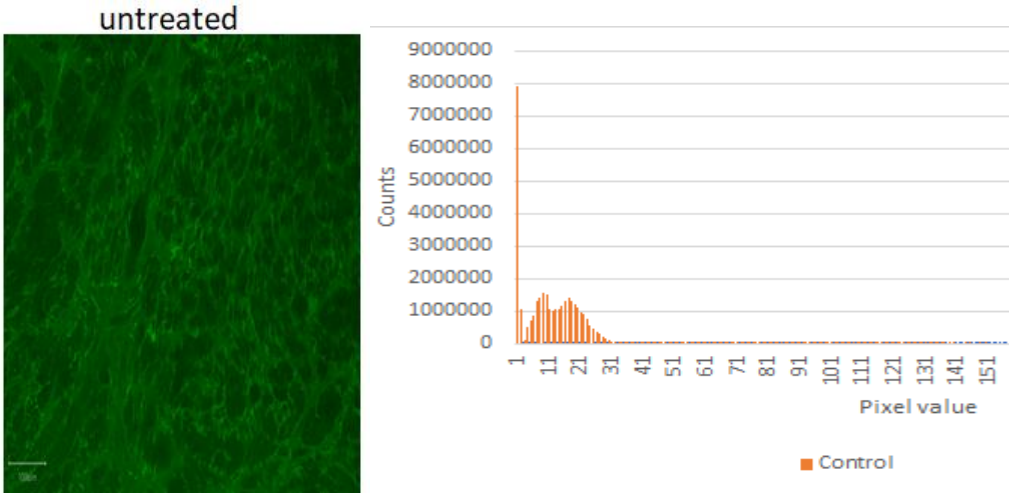

Figure 10. c. Fluorescence image showing quenching of background autofluorescence using Sudan Black B solution (20x magnification). The green channel represents Fluozin-3 zinc dye signal and background fluorescence. untreated is a control slide without Sudan Black B incubation. corresponding image histogram showing pixel intensity distribution.

Table 3: calculation of signal-to-noise ratio of the different Sudan Black B dye in 70% isopropanol incubation time with FluoZin-3 zinc indicator dye.

Sudan Black B incubation time (minutes)	Signal-to-noise ratio
0	0.73
10	1.25
30	1.23
60	0.95
Untreated sample (control)	0.93
Sudan Black B in 70% Ethanol	1.16

3.1.1. Solvent optimization for Sudan Black B

Sudan Black B is more soluble in organic solvent than in aqeuous solutions. The solvent for Sudan Black B was optimized by using ethanol instead of isopropanol. Sudan Black B in 70% ethanol was found to be successful in reducing background autofluorescence in previuos reports [46-49].

Ethanol is more polar and a better solvent than isopropanol for Sudan Black B dye. As observed in our experiment, ethanol dissolves Sudan Black B dye better than isopropanol with less residue after filtration. Ethanol was used instead of isopropanol in anticipation of a different outcome (specific signal preservation). However, Sudan Black B preparation in 70% ethanol resulted in an image with a

lower signal-to-noise ratio than the corresponding incubation time of 30 minutes in 70% isopropanol as shown in Table 3. The specific Fluozin-3 zinc dye signal was also impacted by the Sudan black B in 70% ethanol, but to a lesser extent than in 70% isopropanol (Figure 11). However, the image is also characterised by background fluorescence. The distribution of the pixels in the image histogram is concentrated at the lower pixel values of the dynamic range. Hence the fluorescence image appear dark.

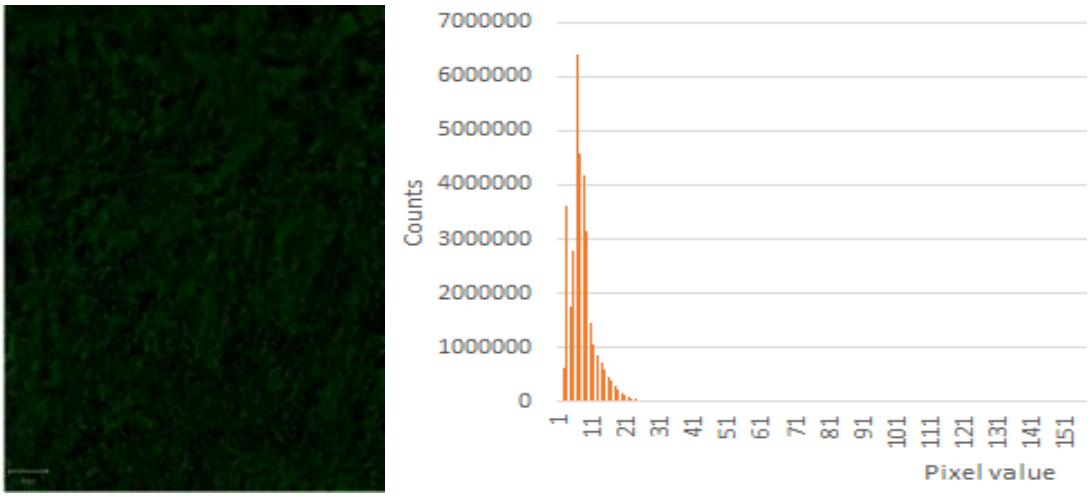

Figure 11. Schematic image showing Sudan Black B solvent optimization (20x magnification) and corresponding image histogram showing distribution of pixel intensity. The green channel represents prostate tissue stained with fluozin-3 zinc probe. Scale: 100 µm.

Background autofluorescence is caused by the presence of endogenous molecules and proteins in cells and tissues [50]. These molecules or proteins fluoresce when excited by light energy of suitable wavelength [50]. Background fluorescence can also be caused by non-specific binding of secondary antibody and aldehyde fixative used for fixing tissue [46]. Several approaches have been used to quench background fluorescence, these include the use of Trypan blue, Pontamine sky blue, Copper (II) sulphate, Sudan Black B in 70% ethanol, Sodium borohydride and a combination of ammonia and ethanol.

Sudan Black B is a diazo dye. It is poorly soluble in water and highly soluble in organic solvents. It quenches autofluorescence due to its ability to absorb light (autofluorescence) and therefore scatter or absorb light arising from histological samples [49]. Sudan Black B reduces or eliminates autofluorescence by obscuring the autofluorescence structure without any chemical reaction [46].

In our experiment, Sudan Black B solution treatment of tissue reduced the specific fluorescence staining intensity. This is consistent with findings in a previous report, where Sudan black B also

reduced specific fluorescence signal [48]. The specific fluorescence signal reduction was said to be caused by the destruction of intracellular structures by organic solvent used in Sudan Black B dissolution [49]. In our experiment, images obtained from Sudan Black B treatment of tissues also contained dark particles. These dark particles may be due to differences in solubility of Sudan Black B in organic solvent and other aqueous solution such as phosphate buffered saline (PBS) used in washing tissue during the staining protocol. The Sudan Black B in 70% ethanol may precipitate into the PBS after washing and thus suspend in the PBS affecting the image quality [49]. It was also discovered that pretreatment with Sudan Black B solution before fluorescence staining significantly reduced specific signal intensity of the fluorescence staining compared to Sudan Black B treatment after fluorescence staining [48]. However, in our experiment, tissues were pretreated with Sudan Black B solution prior to fluorescence staining. This could be another reason for the reduction in the specific fluorescence signal intensity.

The change of solvent to ethanol in our experiment, for Sudan Black B preparation was not successful in preserving the specific fluorescence signal but does slightly reduce background fluorescence and therefore inconsistent with previous report [46].

3.2 TrueBlack autofluorescence quenching test

The treatment of tissue samples with Sudan Black B dye in 70% isopropanol and ethanol resulted in fluorescence images with less background fluorescence. However, the specific signal observed from staining the tissues with Fluozin-3 zinc dye was impacted. Attempting to minimize this effect and further eliminate autofluorescence, TrueBlack autofluorescence quencher was tested. A tissue sample treated with 1X TrueBlack solution in 70% ethanol and a control tissue sample without TrueBlack treatment was used. A comparison of the fluorescence images obtained show that autofluorescence was reduced in the green channel (FITC) and red channels (CY3) of the tissue sample treated with TrueBlack solution (Figure 12a). TrueBlack reduction of autofluorescence in the treated prostate tissue was also evidence when the 3 channels (DAPI/FITC/CY3) were merged (Figure 12b).

TrueBlack Autofluorescence quencher is a reagent that is used to mask lipofuscin autofluorescence and other background fluorescence in tissue sections prior to or after fluorescence staining [51]. It has been reported that Sudan Black B introduces some background fluorescence at certain wavelengths in the red and far-red channels [47, 51]. However, the use of TrueBlack reagent blocks autofluorescence giving minimal background fluorescence in the red and far-red channels [51].

(a)

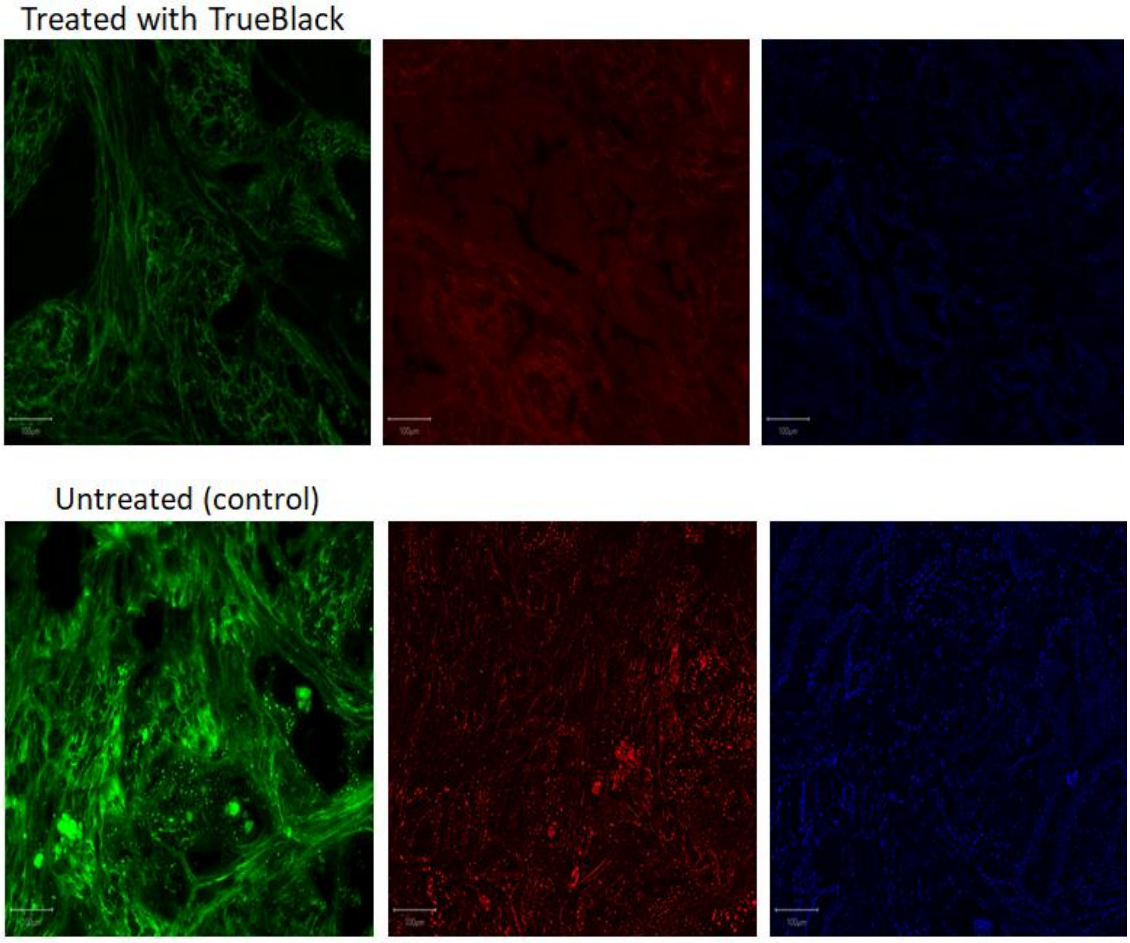

(b)

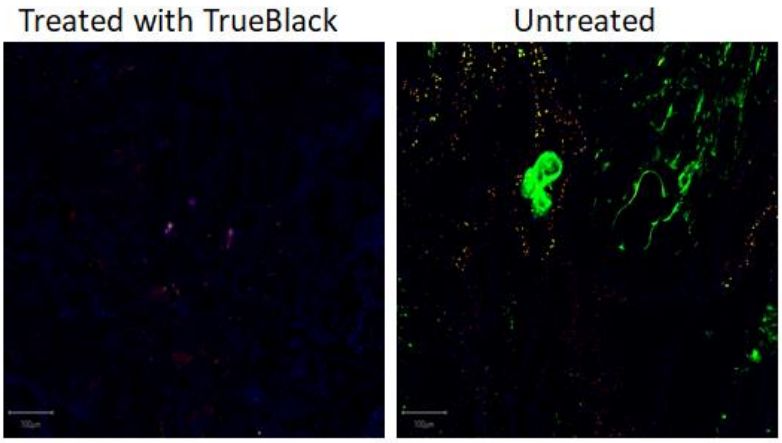

Figure 12. Fluorescence image showing TrueBlack solution quenching of autofluorescence. (a) shows reduction in autofluorescence in the FITC and CY3 channels of prostate tissue treated with TrueBlack solution. (b) show autofluorescence in the merged channels of prostate tissue not treated with Trueblack solution and reduced in the tissue treated with TrueBlack solution. Scale bar= 50 µm

3.3 Single staining of zinc without fixation

The FluoZin-3 zinc indicator dye was tested on PCa tissues without fixing the tissue with 4% paraformaldehyde solution to avoid extra washing steps after fixation. It was suspected that the fixation step and subsequent washings might lead to zinc been washed out of the tissue. This was said to be the case during experimental study in our group using laser ablation inductively coupled plasma mass spectrometry imaging (LA-ICP MSI) to detect zinc in PCa tissue.

A comparison between fixed and unfixed tissue (figure 13) show similarity between both fluorescence images. Therefore, unfixing the tissue did not improve the detection of zinc in tissues by FluoZin-3 zinc indicator dye.

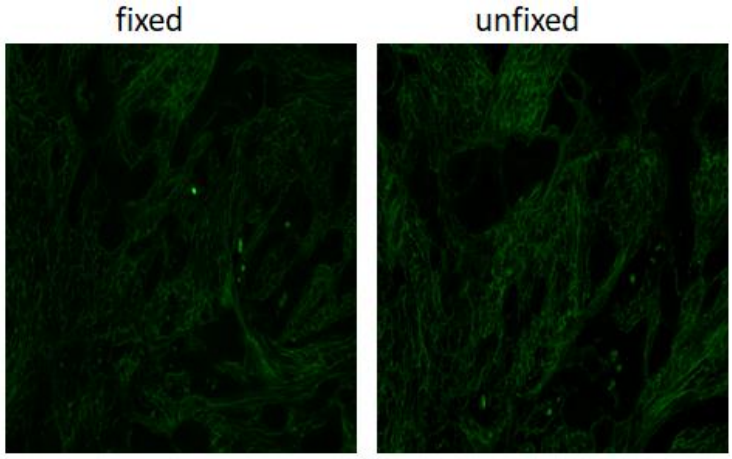

Figure 13. Fluorescence images showing single staining of zinc without fixation. A fixed tissue section was used as a control. Green channel represents Fluozin-3 zinc indicator stained tissue.

3.4 Single staining of zinc with permeabilization of tissue

In our previous experiments, the reduction in specific fluorescence signal was ascribed to Sudan Black B treatment of tissue sections prior to fluorescence staining. However, it was also suspected that less amount of Fluozin-3 zinc indicator dye reached intracellular compartment of cells leading to insufficient fluorescence signal. Fluozin-3 zinc dye is a cell permeant, but it was suspected it did not make the cells permeable enough, to allow its passage into the cells. Thus, permeabilization was performed in tissue sections prior to fluorescence staining. The tissues were permeabilized with TrueBlack Background Blocking Buffer to make the tissue permeable to molecules or ions.

Examination of the fluorescence images shows the presence of weak zinc staining (green spots) and reduction in autofluorescence in permeabilized tissue compared to tissue not permeabilized (figure 14). The reduction in autofluorescence is ascribable to the treatment of the tissue with TrueBlack Background Blocking Buffer and TrueBlack solution in 70% ethanol.

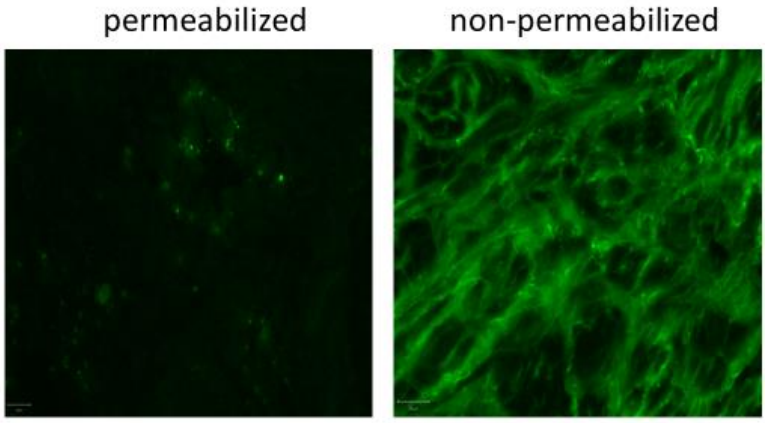

Figure 14. fluorescence images showing permeabilized and non-permeabilized tissue (20X magnification). The green spots in the image of permeabilized tissue indicates staining of zinc with FluoZin-3 zinc dye. Scale bar= 10 µm.

Previous report has shown that other zinc indicator dyes such as New Port Green DCF (NPG) and N-(6-methoxy-8-quinolyl)-p-toluenesulfonamide (TSQ) have been used to determine zinc concentration in PCa tissues simultaneously. The protocol was based on the principle that both zinc indicator dyes detect zinc concentration in tissues due to their differential binding affinity and detection limit for zinc [21]. Thus, the zinc content of the glands and stroma portion of the prostate were determined by a combination of both zinc indicator dyes. It also appears the zinc indicator dyes had the capacity to penetrate the cells due to prolonged incubation (overnight) as the protocol did not include a permeabilization step. However, the protocol did not mention if or how background fluorescence was blocked. Therefore, it is plausible that the observed fluorescence signal after staining, is a combination of the specific signal and background fluorescence.

3.5 Blocking protein binding sites by optimizing Bovine serum albumin incubation times

Bovine serum albumin (BSA) was used to block protein-binding sites in the tissue to prevent antibody from binding non-specific proteins. This blocking step reduces background fluorescence due to unspecific binding. BSA was used to block tissue before incubation with primary antibody (ZIP1 antibody ThermoFisher). The blocking process was optimized to determine the incubation time that

will give the highest SNR and staining intensity using the same antibody dilution (1:400) at 3 different incubation times (0, 10 and 30 minutes were tested to determine the optimal incubation time). Examination of the images indicates the presence of staining in the tissue (figure 15a). The staining was more intense in the stroma than in the epithelia cells of the glands. The staining comprises clusters of spots that are not evenly distributed in the tissue. The clusters of spots have a potential cytosolic sub-cellular localization.

The average intensity and SNR values were calculated as described in section 2.3.1 and 2.3.2 respectively and presented in table 4. The fluorescence mean intensity represents the average intensity of each cell detected in the stained tissue. This average intensity corresponds to the fluorescence observed in the tissue and correlates with the amount of primary/secondary antibody dye bound to the tissue. A comparison of the calculated average intensity shows that incubation with blocking solution (BSA) at 0 minutes had a higher average intensity and SNR values than other incubation times tested. This is unexpected, because at 0 minutes the tissue was incubated in blocking solution and quickly washed off. An explanation for this might be that the protein binding sites in the tissue were yet to be saturated at 0 minutes before washing. And this may have resulted in non-specific antibody binding. However, the average intensity and SNR value decreased significantly at 10 minutes incubation time and increased again at 30 minutes incubation time. The Isotype control used as a negative control for the primary antibody indicates differences in both images. Implying, less non-specific binding by the ZIP1 antibody and thus, there is less background staining.

The distribution of the pixel values for both ZIP1 antibody dilutions shows that the pixels are not evenly distributed as shown in the histogram (figure 15b). The distribution of the pixel values also tends to be concentrated on the right side (lower end of the dynamic range) of the image histogram. This explains the lower image contrast observed.

(a)

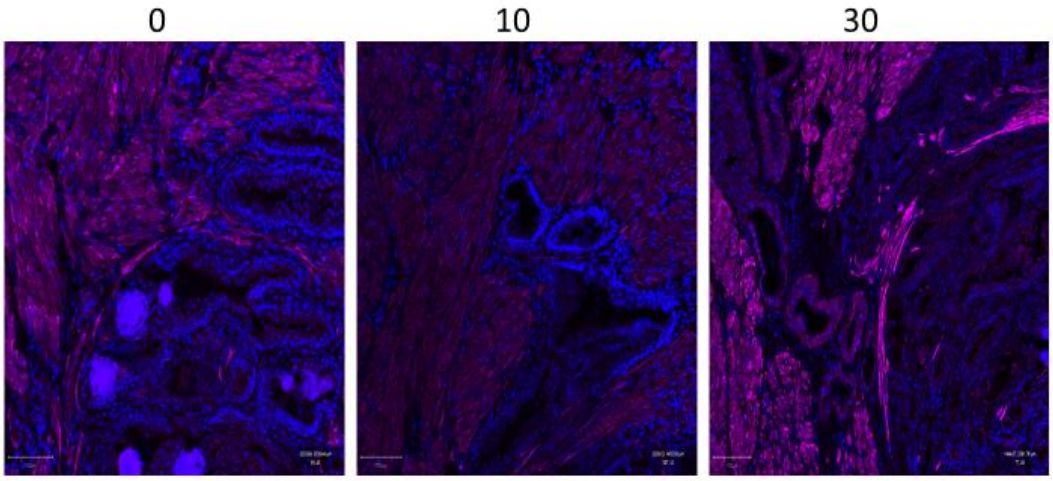

(b)

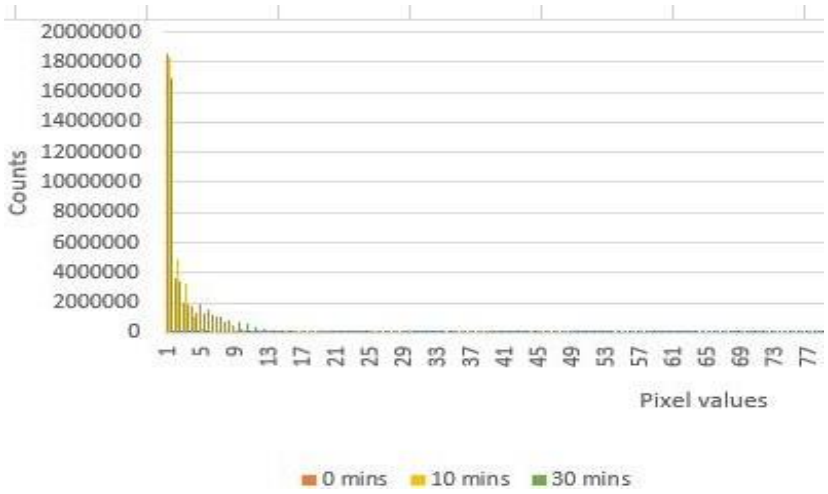

Figure 15. Fluorescence image (20X magnification) showing optimization of bovine serum albumin (BSA) incubation times used for blocking protein binding sites. a. prostate tissues labeled with ZIP1 antibody (1:400) (far-red) and nuclear DNA (blue) after blocking for 0, 10 and 30 minutes respectively with 1% BSA. (b) image histogram showing pixel distribution. Scale bar= 50 µm.

Table 4. Calculation of average intensity and SNR of tissue sections blocked with 1% BSA.

Incubation time	Average intensity	SNR
0	86.64	2.2
10	65.19	1.6
30	77.31	1.9

a b

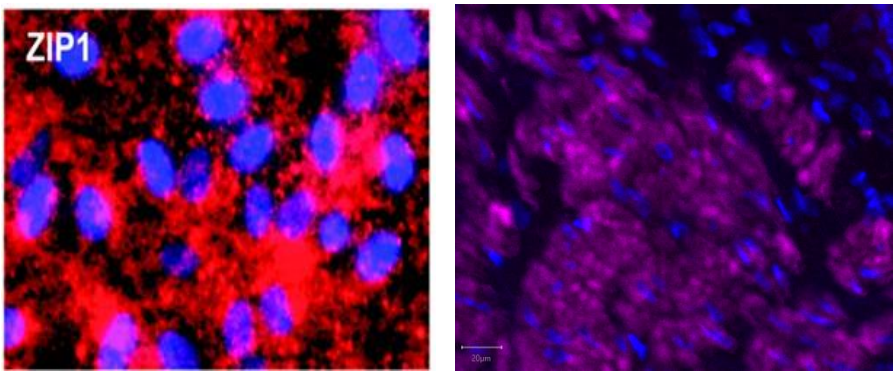

Figure 16. Comparison between fluorescence images of ZIP1 obtained from this test and other source, a. ZIP1 protein labeled with ZIP1 antibody. Taken from Leung et al., 2008 b. ZIP1 protein stained by ZIP antibody (ThermoFisher).

As previously stated, Anti-ZIP1 antibody led to staining characterized by identical intense spots with potential cytosolic localization. The staining pattern expected for Anti-ZIP1 antibody labeling of tissues would be that the labeled ZIP1 proteins localizes to the plasma membrane. However, there seem to be differences in the localization of the labeled proteins observed in this experiment in comparison to the expected sub cellular localization. This may be due to ZIP1 also being localized to intracellular compartments of cells [25].

A comparison of the fluorescence image (figure 16b) obtained from this experiment with images of labeled ZIP1 proteins from previous study (figure 16a) shows differences in distribution and morphology of staining [52]. The staining pattern observed in this experiment comprises clusters of circular intense spots that are not evenly distributed, while the labeled ZIP1 proteins from previous study are granular with almost homogenous distribution.

Bovine serum albumin is a non-reactive protein that blocks non-specific background staining, by blocking hydrophobic interactivity between protein and ionic interactions [53]. The presence of non-specific staining in tissue sections after immunostaining can be reduced by increasing the concentration of bovine serum albumin (BSA). 5% BSA has been used as a blocking solution to improve background signal in a previous report [54]. The increased BSA concentration can also be used as antibody diluent for primary antibody. Incubation of primary antibodies with reagents such as L-cysteine, reduced glutathione, and iodoacetic acid are thought to reduce background staining [53].

3.6. Single staining of RREB1 proteins in prostate tissues

The Anti-RREB1 antibody was optimized by testing two different antibody dilutions on labeled tissues. The fluorescence images obtained (figure 17a) show the presence of staining in the tissues at both dilutions. The staining was more intense at dilution 1:50 and comprises spots. The spots were more at the epithelia cells of the gland than at the stroma. At dilution 1:500, weak staining was observed. Anti-RREB1 antibody dilution 1:50 also had a higher average intensity and SNR compared to 1:500 (Table 5). The pixel distribution of both images is shown in figure 17b. The pixels were distributed in the lower end of the dynamic range of the image histogram.

(a)

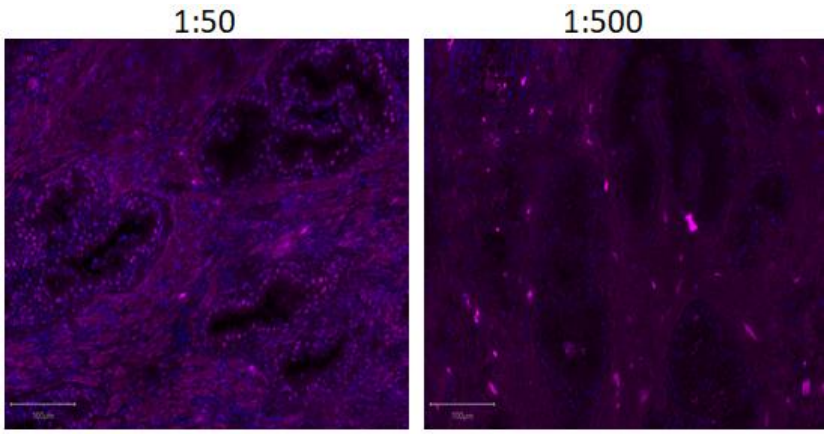

(b)

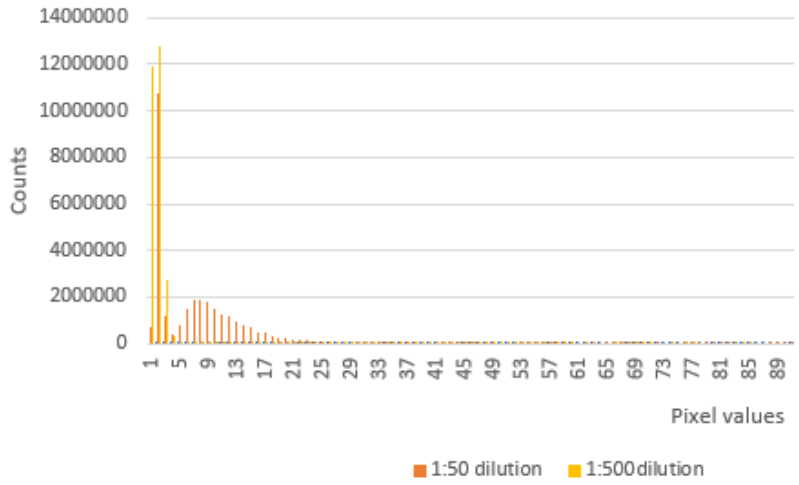

Figure 17. a. Fluorescence image (20X magnification) of prostate tissue incubated in RREB1 antibody (1:50 & 1:500) (far-red channel) and nuclear DNA (DAPI in blue). Higher average intensity and SNR obtained in 1:50 dilution. b. corresponding histogram showing distribution of pixel intensity. Scale bar= 100 µm.

Table 5: calculated average intensity and SNR values for Anti-RREB1 antibody staining.

Antibody dilution	Average intensity	SNR
1:50	92.45	2.3
1:500	32.47	0.8

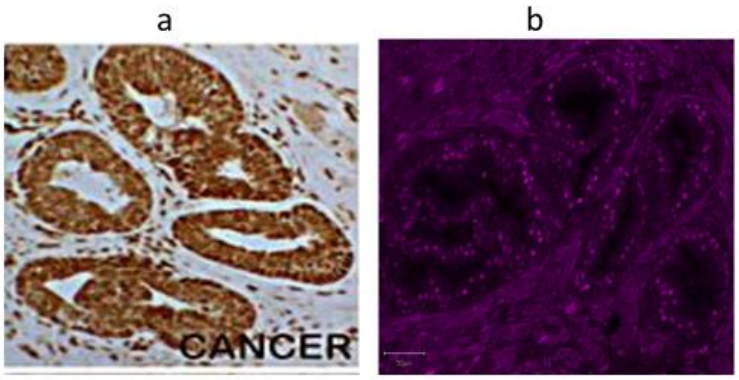

Figure 18. comparison of RREB1 staining from our experiment and other source. a. immunohistochemical staining of RREB1 in prostate tissue section. b. immnuofluorescence staining of RREB1 in prostate tissue section.

RREB1 is a negative regulator of ZIP1 gene expression, implying, an increase in RREB1 expression correlates with a decrease in ZIP1 gene expression. This has been established by previous studies on prostrate cells [30]. Comparing our result with previous studies [30] indicates similarity in the presence of stained RREB1 in the epithelia cells of the prostrate glands (figure 18). However, immunohistochemical staining was used in that experiment compared to immunofluorescence staining used in ours. RREB1 overexpression resulted in decrease in ZIP1 gene expression levels, mostly in the areas of tissue section affected by cancer (figure 18a) [30]. This is a an interesting biological result as RREB1 overexpression is seen close to cancer, thus RREB1 can be made a potential biomarker for prostate cancer development. In our case, it is not known which area of the tissue section is affected by cancer.

RREB1 is expressed in all human tissues except the brain tissue [55]. In addition to prostate cancer, RREB1 overexpression have also been implicated in other diseases such as pancreatic cancer and human diffuse large B cell lymphoma [55]. Overexpressed RREB1 leads to a decrease in zinc levels in PCa by downregulating ZIP1 gene expression.

3.7. Single staining of ZIP1 proteins with Anti-ZIP1 antibody from abcam and Santa Cruz Biotechnology (scbt)

Anti-ZIP1 antibody from abcam and scbt were tested for the single staining of ZIP1 proteins respectively (figure 19 and 20). Antibody dilutions 1:50, 1:100 and 1:500 was tested for Anti-ZIP1 antibody (abcam) (figure 19a and b), while antibody dilutions 1:50 and 1:500 were for tested Anti-ZIP1 antibody from scbt (figure 20a). Assessment of the fluorescence images showed that Anti-ZIP1 antibody (abcam) labeled tissue gave staining characterized by granules with high staining intensity for antibody dilution 1:50 compared to antibody dilutions of 1:100 and 1:500 (figure 19a). The granules were more visible in the epithelia cells of the gland than in the stroma. The granules in the stained tissues were absent in the far-red channel of the unstained tissue (figure 19a). Implying, the ZIP1 antibody is binding a specific target.

Secondary antibody (Anti-Rabbit) only labeled tissue also showed the presence of few stained intense spots (aggregates) in the tissue. Thus, the secondary antibody binds non-specific targets in the tissue sections and therefore indicate presence of some background signals (figure 20b).

The average intensity and SNR values were calculated as stated in sections 2.3.1 & 2.3.2 respectively (Table 6). As shown in Table 6, average intensity decreases as the antibody dilution increases. Antibody dilution 1:50 had the highest average intensity compared to the other dilutions. The average intensities obtained for the different dilutions correlates with the SNR values. Antibody dilution 1:50 also had the higher SNR value compared to others. However, the 1:100 dilution was used for further experiment having given sufficient signal and, also to avoid the risk of unspecific effects due to high antibody concentration.

The pixel value distributions for the Anti-ZIP1 (abcam) are concentrated on the lower end of the dynamic range of the image histogram (figure 19b).

The Anti-ZIP1 antibody (scbt) gave weak staining in the tissue regardless of the antibody dilution tested (figure 20a). The secondary antibody (Anti-Mouse) only labeled tissue did not show staining in the tissue. Hence, the secondary antibody is not binding non-specific targets (figure 20b).

(a)

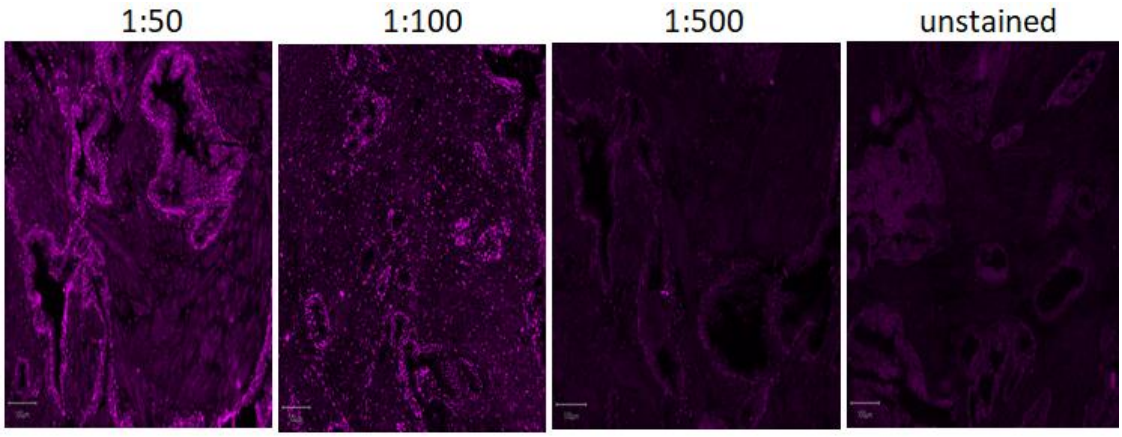

(b)

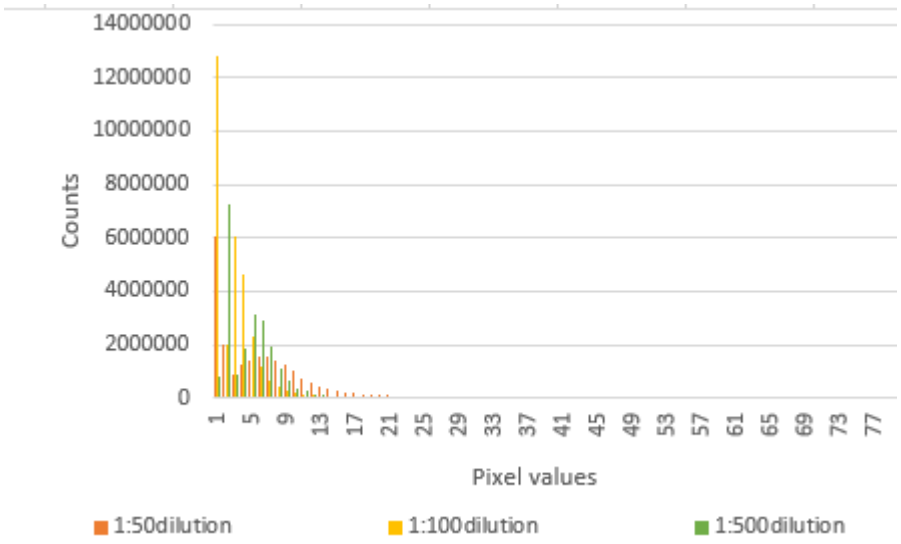

Figure 19. a. Fluorescence image showing ZIP1 stained with abcam ZIP1 Antibody (far-red) using different antibody dilutions (1:50, 1:100 and 1:500). Also shown is far-red channel of tissue not stained with Anti-ZIP1 antibody. Scale bar-=100 µm, magnification= 20X. b. corresponding pixel intensity distribution.

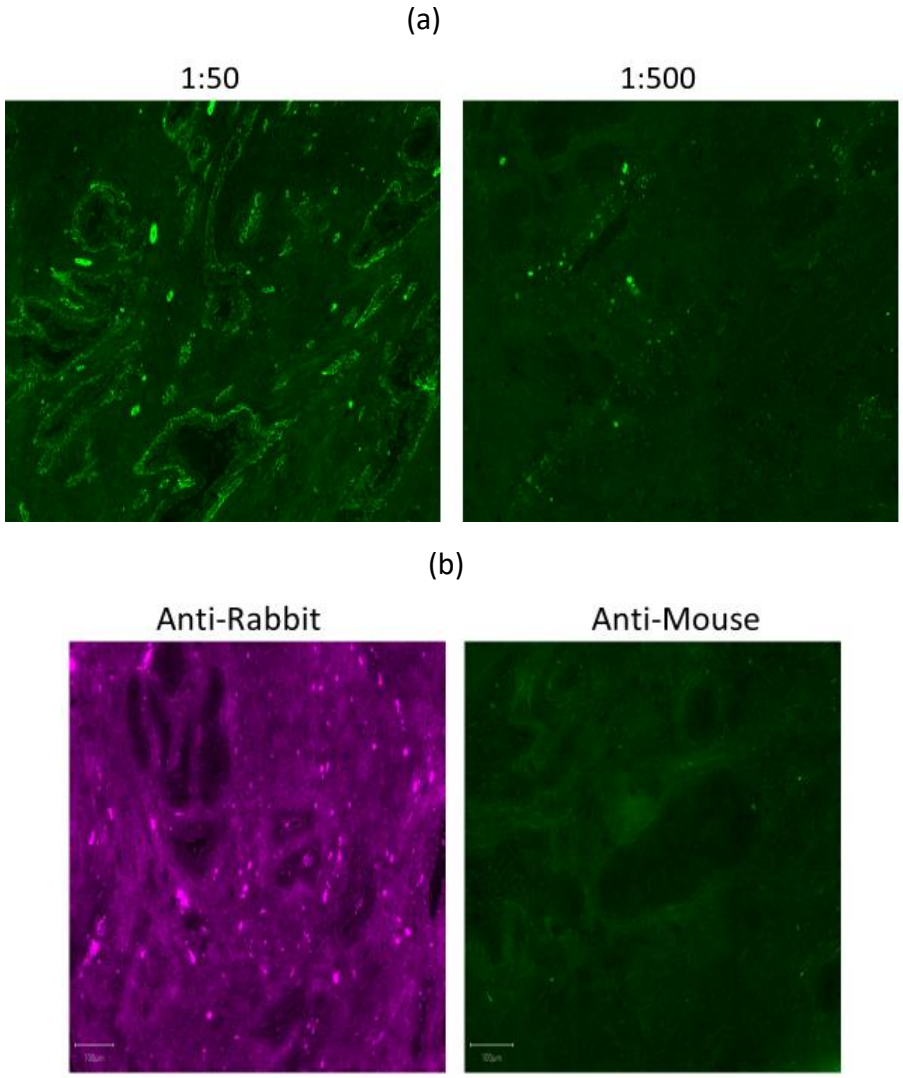

Figure 20. a. Fluorescence image of ZIP1 proteins stained with Anti-ZIP1 antibody from scbt (green channel) using two dilutions. b. labeled prostate tissues with secondary antibodies only (control) Anti-Rabbi secondary antibody (far-red channel), Anti-Mouse secondary antibody (green channel). Scale bar= 100 µm magnification (20x).

Table 6. Calculated average intensity and SNR values for ZIP1 antibody (abcam) for single staining of ZIP1 proteins.

ZIP1 antibody dilution	Average intensity	SNR values
1:50	357.2	8.9
1:100	134.5	3.4
1:500	43.8	1.1

ZIP1 exists in two isoforms (I and II). The Anti-ZIP1 antibody (ThermoFisher) used in this study only recognizes extracellular isoform I of ZIP1. The Anti-ZIP1 antibody (abcam) recognizes both isoform I and II of ZIP1 while ZIP1 antibody from scbt also recognizes isoform I. Comparison of the fluorescence

images of labeled tissues obtained for the ZIP1 antibodies showed that different staining patterns were observed as stated in the respective results sections. However, the staining pattern for ZIP1 antibody (ThermoFisher) consist of some identical spots observed in the secondary antibody (Anti-Rabbit) only labeled tissue. These background staining may have been reduced or eliminated by the TrueBlack solutions used in the test for Anti-ZIP1 antibody (abcam) as 1% BSA proved insufficient in blocking non-specific targets in our previous experiment. The background signal observed when tissue was labeled with secondary antibody only without the primary antibody, may be due to the binding of endogenous Fc receptors as previously reported [53, 54]. Fc receptors are structures found on some cell surfaces and it binds the Fc fragments of antibodies [53]. Furthermore, these background signals are said to be clusters formed by secondary antibody which is caused by its trimeric structure [54].
The staining pattern for ZIP1 antibody (Thermo Fisher) was mostly observed in the stroma than in the glands. While the staining for abcam ZIP1 antibody was mostly in the glands.

3.8 Double staining of ZIP1 and RREB1 in prostate tissues.

ZIP1 and RREB1 proteins were double stained in the tissue to determine their co-localization and distribution in the tissue. Examination of the image indicates the staining pattern for RREB1 proteins (far-red channel) (figure 21) is consistent with the staining observed in figure 17a. The staining was observed in the epithelial cells of the glands and comprises identical spots. The spots indicate the presence of RREB1 staining as this is comparable to the staining obtained in figure 17a. Surprisingly, the green channel which represents ZIP1 protein visualization was characterized by autofluorescence, despite the use of TrueBlack solutions. Thus, the specific signal was indistinguishable from the autofluorescence. What could possibly make the TrueBlack reagents used in quenching autofluorescence less effective in the green channel? An explanation could be that the tissue sections possibly dried out after washing, prior to TrueBlack treatment or the incubation time used for TrueBlack autofluorescence treatment was too long. Thus, affecting the fluorescence staining. However, it is worth mentioning, most of the tissue cores used in our experiments consists of significantly high autofluorescence in the green channel.

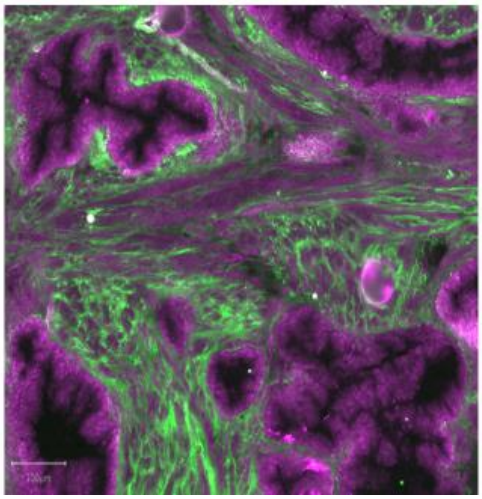

Figure 21. Fluorescence image of double stained ZIP1 and RREB1 proteins in prostate tissue (20X) showed similar staining as compared to the single staining of individual proteins. Tissue stained with ZIP1 (green) and RREB1 antibody (far-red).

4. Conclusion

Intracellular zinc detection in tissues by FluoZin-3 zinc indicator dye had limitations for its use in zinc detection in this study. This may be due to a number of factors such as inability of the zinc indicator dye to penetrate the cell membrane and enter the intracellular cell compartment despite being a cell permeant, also zinc may have been washed out of the tissues during fixation step and subsequent washings. However,I attempted to optimize staining with Fluozin-3 zinc indicator by avoiding tissue fixation and result indicates staining tissue without fixation did not improve zinc detection. But permeabilization of the tissue before staining of zinc did give a weak zinc staining in the tissue. Therefore, this gave credence to our suspicion that less amount of the zinc indicator dye entered the cell and thus the extra permeabilization step is needed to optimize the use of Fluozin-3 zinc indicator dye.

Apart from fluorescence methods, matrix assisted laser desorption ionization mass spectrometry imaging (MALDI-MSI) and laser ablation inductively coupled plasma mass spectrometry imaging (LA-ICP-MSI) can also been used to detect zinc in prostate tissues. But it has limitations due to the time aspect of analyzing large scale cohorts of prostrate tissue for validating the capacity of zinc and ZIP1/RREB1 to be biomarkers for use in clinics. However, LA-ICP-MSI is a perfect tool for validating the staining protocols and compare quantification which is performed using the mass spectrometry method.

The immunolabeling of the tissues for ZIP1 and RREB1 proteins showed signal detections in the tissue, of which the morphologies of the stained proteins were in the form of granules and spots. However, it is not known if the detected signals are specific for the proteins. To determine if the signals detected by the primary antibody is specific for the proteins, cells that are known not to contain the target proteins (knockout cells) should be stained.

In furtherance of the fluorescence method for zinc detection, other zinc indicator dyes such as New Port Green and TSQ zinc indicator dyes can be tested. However, the staining protocol should include a background fluorescence quenching step and the use of image analysis software to determine the stain quality rather than physical observation as used in the previous report.

The ZIP1 gene expression can be determined by qRT-PCR to quantify ZIP1 expression levels and how it correlates with zinc concentration/distribution levels. Also, abundance of RREB1 and ZIP1 proteins can be determined by western blot to determine their correlation and how this affect zinc levels in prostate tissue. Furthermore, a higher dilution of the Anti-Rabbit secondary antibody could be tested to reduce the background signal as it appears to form some aggregates.

As previously mentioned, the current screening tools for early stage PCa diagnosis has limitations. Therefore, alternative procedures for PCa diagnosis are imperative. Various reports have confirmed

zinc to be depleted in PCa and different fluorescence-based methods have been used to detect zinc in PCa tissues. Therefore, fluorescence method (Zinc indicator dyes) of zinc detection in PCa can be applied to clinical samples. Needle-biopsy prostate tissue cores obtained from patients can be analyzed by fluorescence staining to determine zinc concentrations in the tissues. Thus, this method of PCa detection has the advantage of determining the grade and cancer location.

RREB1 should be investigated further in a larger study of prostate cancer patients, as it can be a potential biomarker for PCa development and therefore a target for drugs.

5. References

1. Bray, F., et al., *Global cancer statistics 2018: GLOBOCAN estimates of incidence and mortality worldwide for 36 cancers in 185 countries.* CA Cancer J Clin, 2018. **68**(6): p. 394-424.

2. *Cancer in Norway, 2018. Retrieved from Cancer Registry of Norway:* https://www.kreftregisteret.no/en/General/Publications/Cancer-in-Norway/cancer-in-norway-2018.

3. Franz, M.C., et al., *Zinc transporters in prostate cancer.* Molecular aspects of medicine, 2013. **34**(2-3): p. 735-741.

4. Cabarkapa, S., et al., *Prostate cancer screening with prostate-specific antigen: A guide to the guidelines.* Prostate international, 2016. **4**(4): p. 125-129.

5. Costello, L.C., R.B. Franklin, and P. Narayan, *Citrate in the diagnosis of prostate cancer.* Prostate, 1999. **38**(3): p. 237-45.

6. Loeb, S., et al., *Overdiagnosis and overtreatment of prostate cancer.* European urology, 2014. **65**(6): p. 1046-1055.

7. Heijnsdijk, E.A.M., et al., *Quality-of-life effects of prostate-specific antigen screening.* The New England journal of medicine, 2012. **367**(7): p. 595-605.

8. Klotz, L., *Prostate cancer overdiagnosis and overtreatment.* Curr Opin Endocrinol Diabetes Obes, 2013. **20**(3): p. 204-9.

9. Costello, L.C. and R.B. Franklin, *A comprehensive review of the role of zinc in normal prostate function and metabolism; and its implications in prostate cancer.* Arch Biochem Biophys, 2016. **611**: p. 100-112.

10. Schipper, R., et al., *Polyamines and prostatic cancer*. Vol. 31. 2003. 375-80.

11. McNeal, J.E., *Normal histology of the prostate.* Am J Surg Pathol, 1988. **12**(8): p. 619-33.

12. Kolenko, V., et al., *Zinc and zinc transporters in prostate carcinogenesis.* Nature reviews. Urology, 2013. **10**(4): p. 219-226.

13. Bafaro, E., et al., *The emerging role of zinc transporters in cellular homeostasis and cancer.* Signal Transduction And Targeted Therapy, 2017. **2**: p. 17029.

14. Chasapis, C.T., et al., *Zinc and human health: an update.* Archives of Toxicology, 2012. **86**(4): p. 521-534.

15. Yuan, N., et al., *Effects of exogenous zinc on the cellular zinc distribution and cell cycle of A549 cells.* Biosci Biotechnol Biochem, 2012. **76**(11): p. 2014-20.

16. Vallee, B.L. and K.H. Falchuk, *The biochemical basis of zinc physiology.* Physiol Rev, 1993. **73**(1): p. 79-118.

17. Gumulec, J., et al., *Serum and tissue zinc in epithelial malignancies: a meta-analysis.* PLoS One, 2014. **9**(6): p. e99790.

18. Feng, P., et al., *Direct effect of zinc on mitochondrial apoptogenesis in prostate cells.* Prostate, 2002. **52**(4): p. 311-8.

19. Franklin, R.B. and L.C. Costello, *Zinc as an anti-tumor agent in prostate cancer and in other cancers.* Arch Biochem Biophys, 2007. **463**(2): p. 211-7.

20. Mawson, C.A. and M.I. Fischer, *The occurrence of zinc in the human prostate gland.* Can J Med Sci, 1952. **30**(4): p. 336-9.

21. Johnson, L.A., et al., *Differential zinc accumulation and expression of human zinc transporter 1 (hZIP1) in prostate glands.* Methods, 2010. **52**(4): p. 316-21.

22. Franklin, R.B., et al., *Zinc and zinc transporters in normal prostate and the pathogenesis of prostate cancer.* Front Biosci, 2005. **10**: p. 2230-9.

23. Cortesi, M., et al., *Clinical assessment of the cancer diagnostic value of prostatic zinc: a comprehensive needle-biopsy study.* Prostate, 2008. **68**(9): p. 994-1006.

24. Costello, L.C. and R.B. Franklin, *Cytotoxic/tumor suppressor role of zinc for the treatment of cancer: an enigma and an opportunity.* Expert Rev Anticancer Ther, 2012. **12**(1): p. 121-8.

25. Jeong, J. and D.J. Eide, *The SLC39 family of zinc transporters.* Molecular aspects of medicine, 2013. **34**(2-3): p. 612-619.

26. Franklin, R.B., et al., *Human ZIP1 is a major zinc uptake transporter for the accumulation of zinc in prostate cells.* J Inorg Biochem, 2003. **96**(2-3): p. 435-42.

27. Costello, L.C., et al., *Evidence for a zinc uptake transporter in human prostate cancer cells which is regulated by prolactin and testosterone.* J Biol Chem, 1999. **274**(25): p. 17499-504.

28. Franklin, R.B., et al., *hZIP1 zinc uptake transporter down regulation and zinc depletion in prostate cancer.* Molecular Cancer, 2005. **4**(1): p. 32.

29. Desouki, M.M., et al., *hZip2 and hZip3 zinc transporters are down regulated in human prostate adenocarcinomatous glands.* Mol Cancer, 2007. **6**: p. 37.

30. Zou, J., et al., *hZIP1 zinc transporter down-regulation in prostate cancer involves the overexpression of ras responsive element binding protein-1 (RREB-1).* The Prostate, 2011. **71**(14): p. 1518-1524.

31. Milon, B.C., et al., *Ras responsive element binding protein-1 (RREB-1) down-regulates hZIP1 expression in prostate cancer cells.* Prostate, 2010. **70**(3): p. 288-96.

32. Weber, M.J. and D. Gioeli, *Ras signaling in prostate cancer progression.* J Cell Biochem, 2004. **91**(1): p. 13-25.

33. Gioeli, D., *Signal transduction in prostate cancer progression.* Clin Sci (Lond), 2005. **108**(4): p. 293-308.

34. Im, K., et al., *An Introduction to Performing Immunofluorescence Staining.* Methods Mol Biol, 2019. **1897**: p. 299-311.

35. Ramos-Vara, J.A. and M.A. Miller, *When tissue antigens and antibodies get along: revisiting the technical aspects of immunohistochemistry--the red, brown, and blue technique.* Vet Pathol, 2014. **51**(1): p. 42-87.

36. Donaldson, J.G., *Immunofluorescence Staining.* Curr Protoc Cell Biol, 2015. **69**: p. 4.3.1-4.3.7.

37. Michael McCaffery, J. and M.G. Farquhar, *[29] Localization of GTPases by indirect immunofluorescence and immunoelectron microscopy*, in *Methods in Enzymology*. 1995, Academic Press. p. 259-279.

38. Hermanson, G.T., *Chapter 10 - Fluorescent Probes*, in *Bioconjugate Techniques (Third Edition)*, G.T. Hermanson, Editor. 2013, Academic Press: Boston. p. 395-463.

39. Sanderson, M.J., et al., *Fluorescence microscopy.* Cold Spring Harbor protocols, 2014. **2014**(10): p. pdb.top071795-pdb.top071795.

40. *Enzolifesciences, Technotes 2019. Retrieved from Enzolifesciences:* https://www.enzolifesciences.com/science-center/technotes/

41. Lichtman, J. and J. Conchello, *Fluorescence Microscopy.* Nature methods, 2006. **2**: p. 910-9.

42. Bankhead, P., et al., *QuPath: Open source software for digital pathology image analysis.* Scientific Reports, 2017. **7**(1): p. 16878.

43. Bertilsson, H., et al., *A new method to provide a fresh frozen prostate slice suitable for gene expression study and MR spectroscopy.* Prostate, 2011. **71**(5): p. 461-9.

44. Reimann, C., et al., *Does bottle type and acid-washing influence trace element analyses by ICP-MS on water samples? A test covering 62 elements and four bottle types: high density polyethene (HDPE), polypropene (PP), fluorinated ethene propene copolymer (FEP) and perfluoroalkoxy polymer (PFA).* Sci Total Environ, 1999. **239**(1-3): p. 111-30.

45. Ferrand, A., et al., *Using the NoiSee workflow to measure signal-to-noise ratios of confocal microscopes.* Scientific Reports, 2019. **9**(1): p. 1165.

46. Oliveira, V.C., et al., *Sudan Black B treatment reduces autofluorescence and improves resolution of in situ hybridization specific fluorescent signals of brain sections.* Histol Histopathol, 2010. **25**(8): p. 1017-24.

47. Romijn, H.J., et al., *Double immunolabeling of neuropeptides in the human hypothalamus as analyzed by confocal laser scanning fluorescence microscopy.* J Histochem Cytochem, 1999. **47**(2): p. 229-36.

48. Schnell, S.A., W.A. Staines, and M.W. Wessendorf, *Reduction of lipofuscin-like autofluorescence in fluorescently labeled tissue.* J Histochem Cytochem, 1999. **47**(6): p. 719-30.

49. Qi, L., et al., *Pre-culture Sudan Black B treatment suppresses autofluorescence signals emitted from polymer tissue scaffolds.* Scientific Reports, 2017. **7**(1): p. 8361.

50. Monici, M., *Cell and tissue autofluorescence research and diagnostic applications.* Biotechnol Annu Rev, 2005. **11**: p. 227-56.

51. *Biotium. TrueBlack Lipofuscin Autofluorescence Quencher. Retrieved from Biotium:* https://biotium.com/product/trueblack-lipofuscin-autofluorescence-quencher/

52. Leung, K.W., et al., *Expression of ZnT and ZIP zinc transporters in the human RPE and their regulation by neurotrophic factors.* Invest Ophthalmol Vis Sci, 2008. **49**(3): p. 1221-31.

53. Buchwalow, I., et al., *Non-specific binding of antibodies in immunohistochemistry: fallacies and facts.* Sci Rep, 2011. **1**: p. 28.

54. Axelrod, H.D., K.J. Pienta, and K.C. Valkenburg, *Optimization of Immunofluorescent Detection of Bone Marrow Disseminated Tumor Cells.* Biological procedures online, 2018. **20**: p. 13-13.

55. Deng, Y.N., et al., *Transcription Factor RREB1: from Target Genes towards Biological Functions.* Int J Biol Sci, 2020. **16**(8): p. 1463-1473.